Figure 2A

Figure 2A

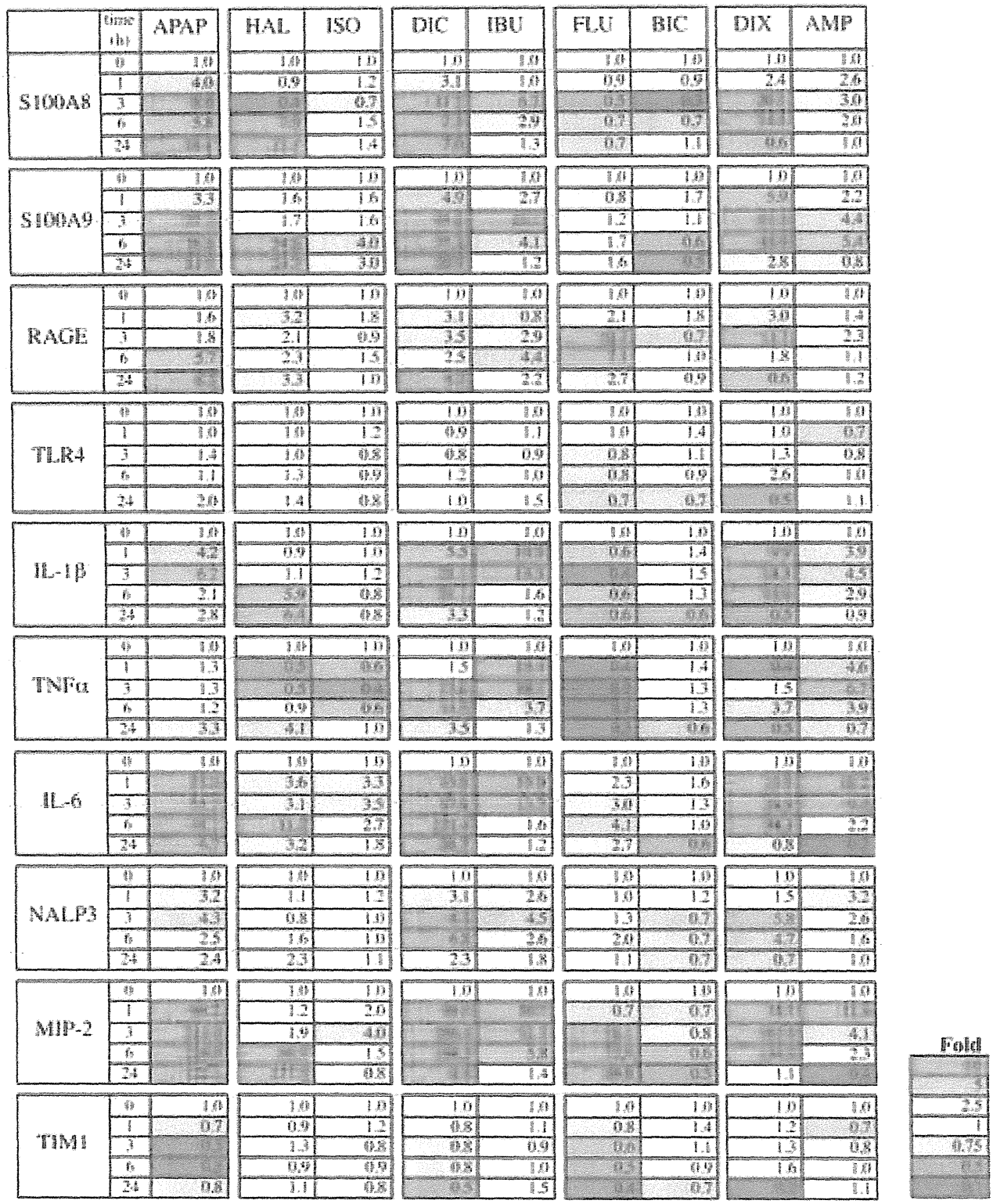

	Time (h)	APAP	HAL	ISO	DIC	IBU	FLU	BIC	DIX	AMP
S100A8	0	1.0	1.0	1.0	1.0	1.0	1.0	1.0	1.0	1.0
	1	4.0	0.9	1.2	3.1	1.0	0.9	0.9	2.4	2.6
	3			0.7						3.0
	6			1.5		2.9	0.7	0.7		2.0
	24			1.4		1.3	0.7	1.1	0.6	1.0
S100A9	0	1.0	1.0	1.0	1.0	1.0	1.0	1.0	1.0	1.0
	1	3.3	1.6	1.6	4.9	2.7	0.8	1.7		2.2
	3		1.7	1.6			1.2	1.1		4.4
	6			3.0		4.1	1.7	0.6		5.4
	24			3.0		1.2	1.6		2.8	0.8
RAGE	0	1.0	1.0	1.0	1.0	1.0	1.0	1.0	1.0	1.0
	1	1.6	3.2	1.8	3.1	0.8	2.1	1.8	3.0	1.4
	3	1.8	2.1	0.9	3.5	2.9		0.7		2.3
	6		2.3	1.5	2.5	4.4		1.0	1.8	1.1
	24		3.3	1.0		2.2	2.7	0.9		1.2
TLR4	0	1.0	1.0	1.0	1.0	1.0	1.0	1.0	1.0	1.0
	1	1.0	1.0	1.2	0.9	1.1	1.0	1.4	1.0	0.7
	3	1.4	1.0	0.8	0.8	0.9	0.8	1.1	1.3	0.8
	6	1.1	1.3	0.9	1.2	1.0	0.8	0.9	2.6	1.0
	24	2.0	1.4	0.8	1.0	1.5	0.7	0.7		1.1
IL-1β	0	1.0	1.0	1.0	1.0	1.0	1.0	1.0	1.0	1.0
	1	4.2	0.9	1.0			0.6	1.4		3.9
	3		1.1	1.2				1.5		4.5
	6	2.1		0.8		1.6	0.6	1.3		2.9
	24	2.8		0.8	3.3	1.2	0.6	0.6		0.9
TNFα	0	1.0	1.0	1.0	1.0	1.0	1.0	1.0	1.0	1.0
	1	1.3			1.5			1.4		
	3	1.3						1.3	1.5	
	6	1.2	0.9			3.7		1.3	3.7	3.9
	24	3.3	4.1	1.0	3.5	1.3		0.6		0.7
IL-6	0	1.0	1.0	1.0	1.0	1.0	1.0	1.0	1.0	1.0
	1		3.6	3.3			2.3	1.6		
	3		3.1	3.5			3.0	1.3		
	6			2.7		1.6	4.1	1.0		3.2
	24		3.2	1.8		1.2	2.7		0.8	
NALP3	0	1.0	1.0	1.0	1.0	1.0	1.0	1.0	1.0	1.0
	1	3.2	1.1	1.2	3.1	2.6	1.0	1.2	1.5	3.2
	3		0.8	1.0			1.3			2.6
	6		1.6	1.0		2.6	2.0			1.6
	24	2.4	2.3	1.1	2.3	1.8	1.1	0.7	0.7	1.0
MIP-2	0	1.0	1.0	1.0	1.0	1.0	1.0	1.0	1.0	1.0
	1		1.2	2.0			0.7	0.7		
	3		1.9	4.0				0.8		4.1
	6			1.5						2.3
	24			0.8		1.4			1.1	
TIM1	0	1.0	1.0	1.0	1.0	1.0	1.0	1.0	1.0	1.0
	1	0.7	0.9	1.2	0.8	1.1	0.8	1.4	1.2	0.7
	3		1.3	0.8	0.8	0.9	0.6	1.1	1.3	0.8
	6		0.9	0.9	0.8	1.0	0.5	0.9	1.6	1.0
	24	0.8	1.1	0.8		1.5		0.7		1.1

Fold

5
2.5
1
0.75

Figure 2B

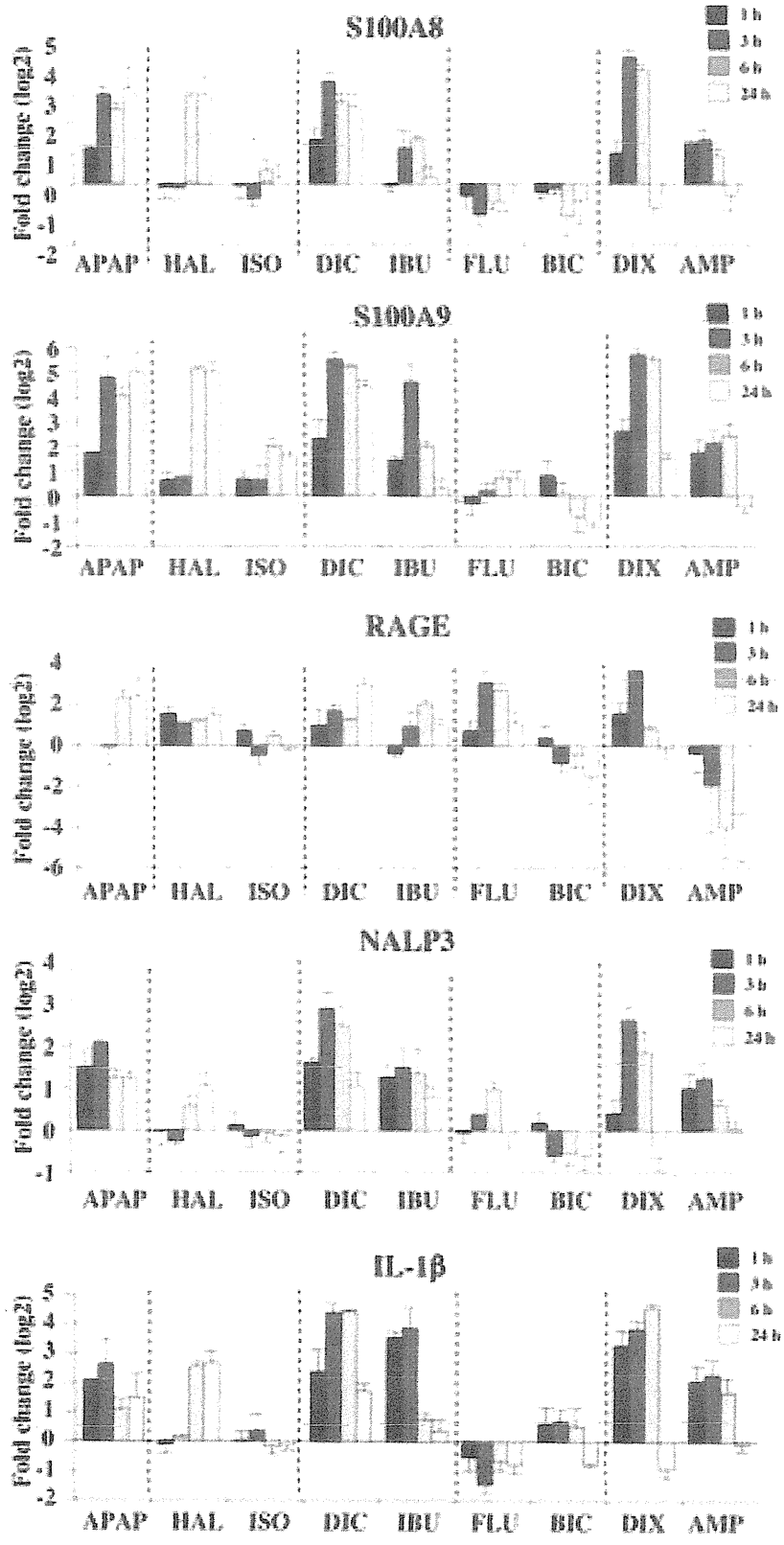
S100A8
S100A9
RAGE
NALP3
IL-1β
Fold change (log2)
1 h
3 h
6 h
24 h
APAP
HAL
ISO
DIC
IBU
FLU
BIC
DIX
AMP

Figure 3

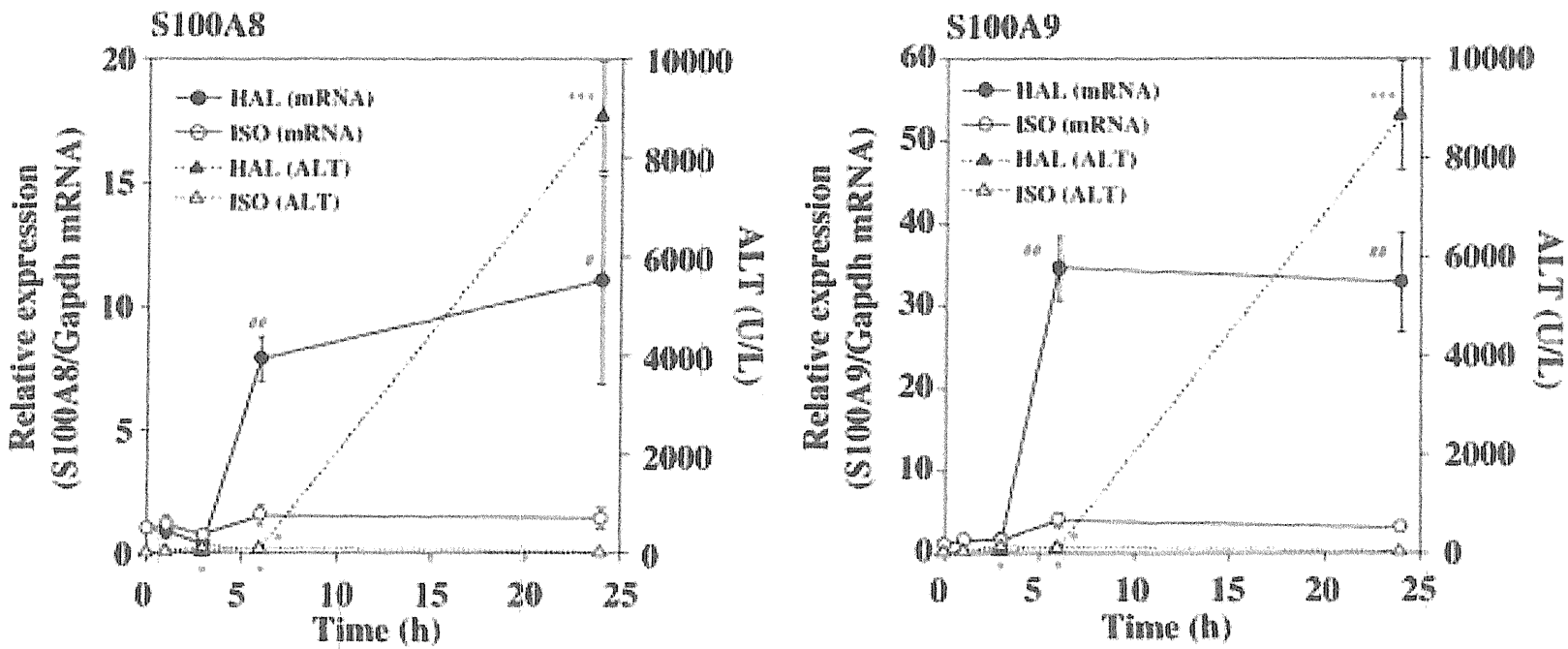
S100A8
Relative expression
(S100A8/Gapdh mRNA)
ALT (U/L)
Time (h)
HAL (mRNA)
ISO (mRNA)
HAL (ALT)
ISO (ALT)
S100A9
Relative expression
(S100A9/Gapdh mRNA)
ALT (U/L)
Time (h)
HAL (mRNA)
ISO (mRNA)
HAL (ALT)
ISO (ALT)

Figure 4

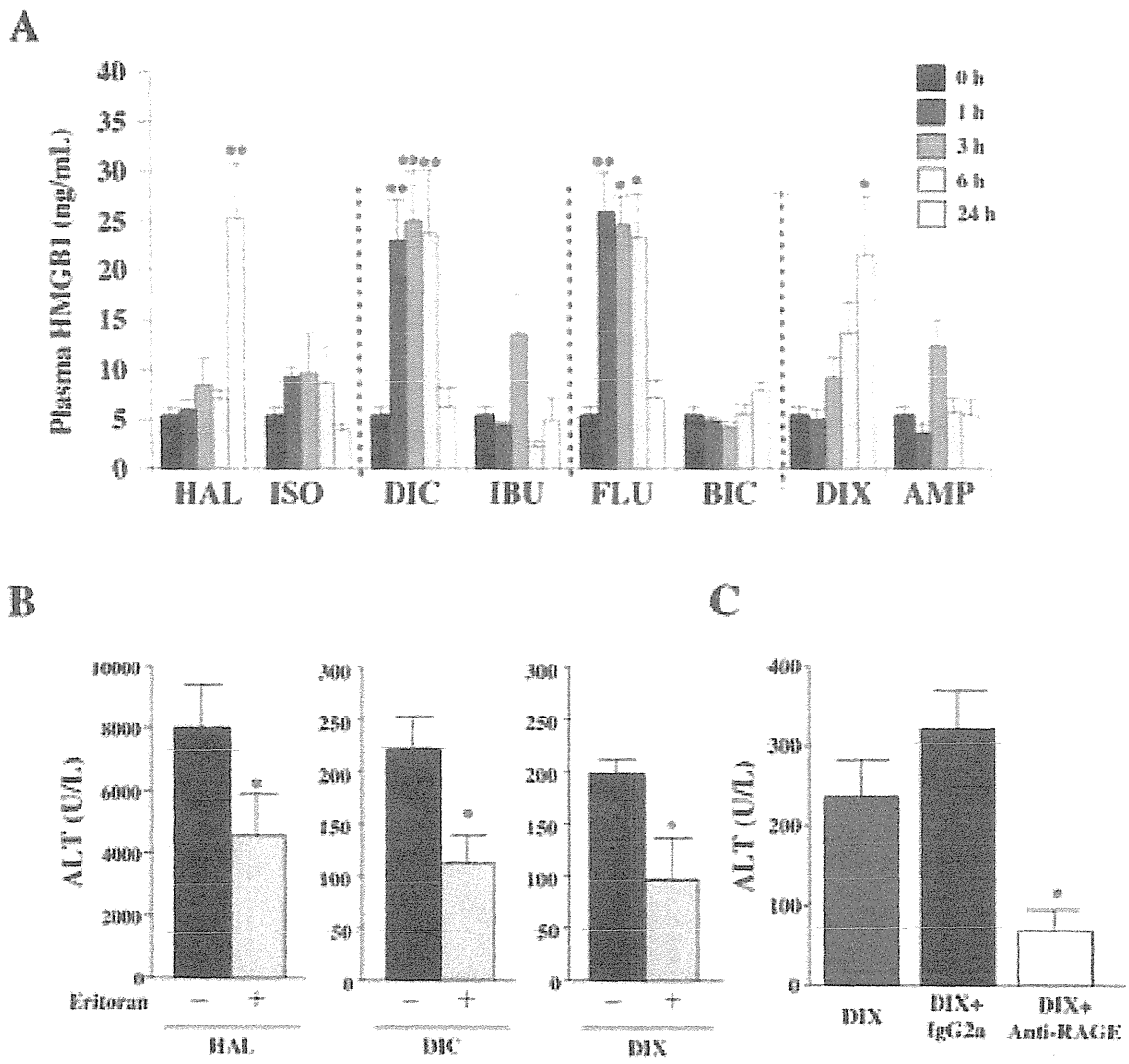
A
Plasma HMGB1 (ng/mL)
0 h
1 h
3 h
6 h
24 h
HAL
ISO
DIC
IBU
FLU
BIC
DIX
AMP
B
ALT (U/L)
Eritoran
HAL
DIC
DIX
C
ALT (U/L)
DIX
DIX+ IgG2a
DIX+ Anti-RAGE

Figure 5

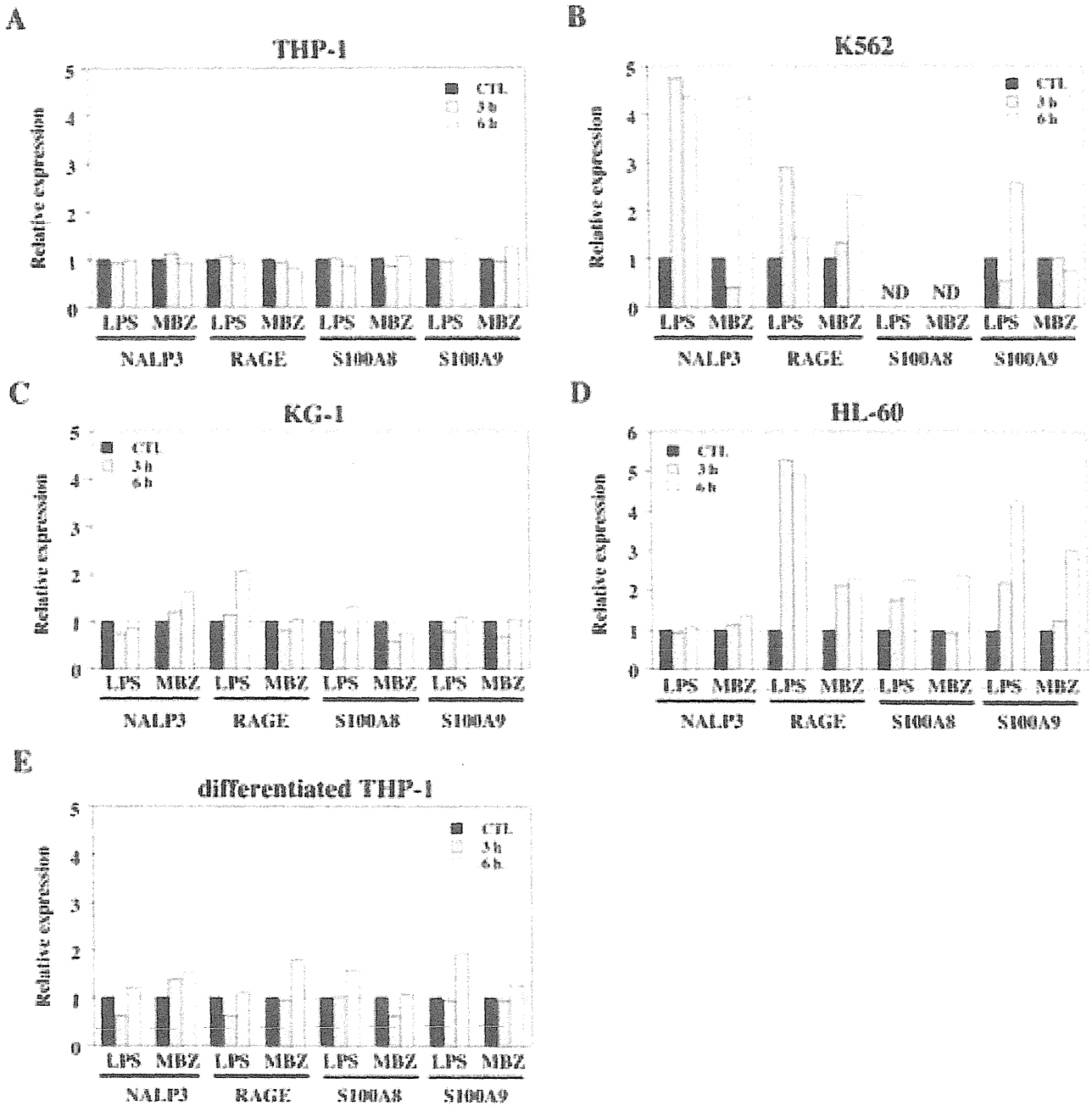
A
THP-1
B
K562
C
KG-1
D
HL-60
E
differentiated THP-1
Relative expression
CTL
3 h
6 h
LPS
MBZ
NALP3
RAGE
S100A8
S100A9
ND

Figure 6

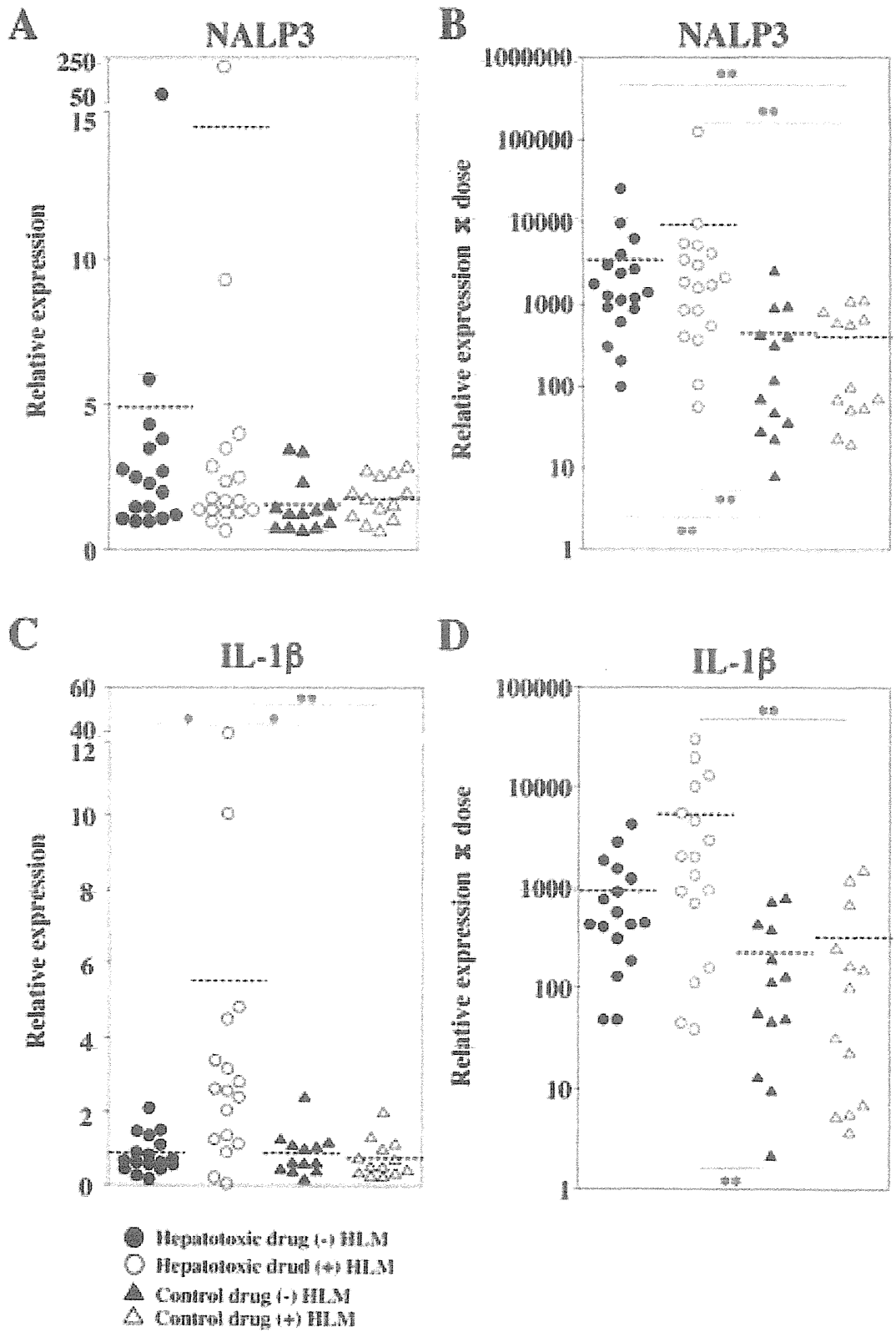
A
NALP3
Relative expression
250
50
15
10
5
0
B
NALP3
Relative expression x dose
1000000
100000
10000
1000
100
10
1
**
C
IL-1β
Relative expression
60
40
12
10
8
6
4
2
0
D
IL-1β
Relative expression x dose
100000
10000
1000
100
10
1
Hepatotoxic drug (-) HLM
Hepatotoxic drud (+) HLM
Control drug (-) HLM
Control drug (+) HLM

Figure 7

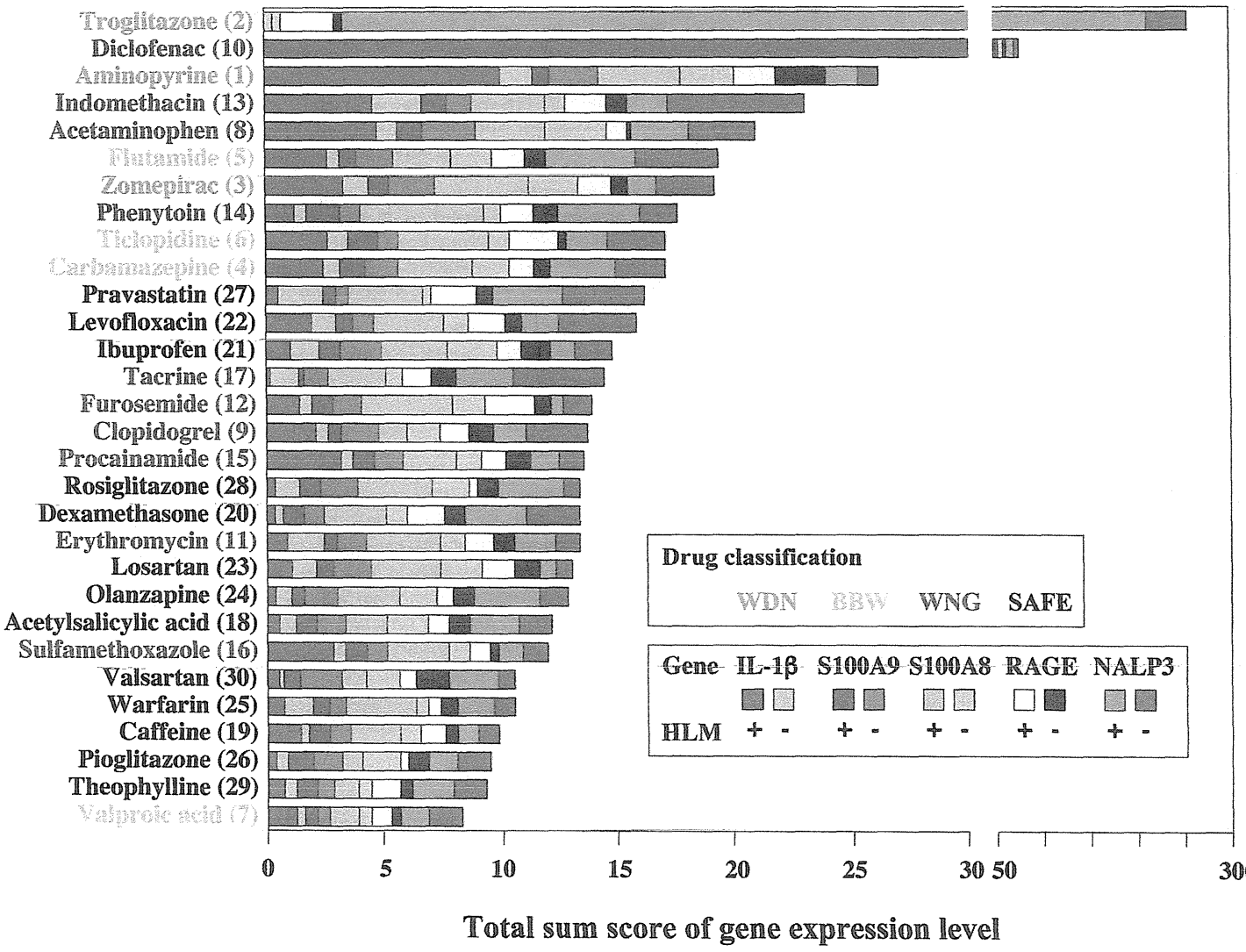
Troglitazone (2)
Diclofenac (10)
Aminopyrine (1)
Indomethacin (13)
Acetaminophen (8)
Flutamide (5)
Zomepirac (3)
Phenytoin (14)
Ticlopidine (6)
Carbamazepine (4)
Pravastatin (27)
Levofloxacin (22)
Ibuprofen (21)
Tacrine (17)
Furosemide (12)
Clopidogrel (9)
Procainamide (15)
Rosiglitazone (28)
Dexamethasone (20)
Erythromycin (11)
Losartan (23)
Olanzapine (24)
Acetylsalicylic acid (18)
Sulfamethoxazole (16)
Valsartan (30)
Warfarin (25)
Caffeine (19)
Pioglitazone (26)
Theophylline (29)
Valproic acid (7)
Drug classification
WDN
BBW
WNG
SAFE
Gene
IL-1β
S100A9
S100A8
RAGE
NALP3
HLM
+ - + - + - + - + -
0
5
10
15
20
25
30
50
300
Total sum score of gene expression level

Research Article

Journal of Applied Toxicology

Received: 17 December 2013, Revised: 3 February 2014, Accepted: 5 February 2014 Published online in Wiley Online Library

(wileyonlinelibrary.com) DOI 10.1002/jat.3002

Involvement of immune- and inflammatory-related factors in flucloxacillin-induced liver injury in mice

Shohei Takai[a], Satonori Higuchi[a], Azusa Yano[a], Koichi Tsuneyama[b], Tatsuki Fukami[a], Miki Nakajima[a] and Tsuyoshi Yokoi[a,c]*

ABSTRACT: Drug-induced liver injury (DILI) is a serious problem in pre-clinical stages of drug development and clinical pharmacotherapy, but the pathogenesis of DILI has not been elucidated. Flucloxacillin (FLX), which is a β-lactam antibiotic of the penicillin class that is used widely in Europe and Australia, rarely causes DILI. Clinical features suggest that FLX-induced liver injury is caused by immune- and inflammatory-related factors, but the mechanism of FLX-induced liver injury is unknown. The purpose of this study was to elucidate the mechanisms of FLX-induced liver injury *in vivo*. Plasma alanine aminotransferase, aspartate aminotransferase and total-bilirubin levels were significantly elevated in FLX-administered mice [1000 mg kg^{-1}, intraperitoneally (i.p.)]. Toll-like receptor 4 (TLR4) ligands, such as high-mobility group box 1 (HMGB1) and S100A8/A9, were significantly increased in FLX-administered mice, and inflammatory factors, such as interleukin (IL)-1β, tumor necrosis factor-alpha (TNF-α), macrophage inflammatory protein (MIP)-2, CXC chemokine-ligand-1 (CXCL1) and monocyte chemoattractant protein (MCP)-1, were also significantly elevated. IL-17-related transcriptional factors and cytokines were increased, and the administration of recombinant IL-17 (2 mg per body weight, i.p.) resulted in an exacerbation of the FLX-induced liver injury. TLR4-associated-signal transduction may be involved in FLX-induced liver injury, and IL-17 is an exacerbating factor. Copyright © 2014 John Wiley & Sons, Ltd.

Keywords: flucloxacillin; inflammatory; toll-like receptor 4 (TLR4); IL-17

Introduction

Drug-induced liver injury (DILI) is the most frequent reason for drug withdrawal from the market and the cessation of new drug development by pharmaceutical companies (Kaplowitz, 2005). Some drugs, such as halothane, diclofenac and methimazole, have been suggested to induce immune- and/or inflammatory-related DILI (Kobayashi *et al.*, 2009, 2012; Yano *et al.*, 2012). The underlying mechanisms of DILI have been largely unknown because of a lack of proper animal models.

There are many clinical drugs that cause DILI. In particular, a large number of antibiotics are known to cause DILI (Verma & Kaplowitz, 2009). Flucloxacillin (FLX) is a semi-synthetic penicillin belonging to the isoxazolyl penicillin family. FLX is used widely and is prescribed for Gram-positive infections such as *Staphylococcus aureus*. FLX-administered patients rarely develop DILI, but some cases result in fatal damage and liver transplantations (Björnsson & Olsson, 2005). This type of FLX-induced liver injury is predominantly cholestasis, and the risk of FLX-induced liver injury is thought to be approximately 8.5 in 100,000 patients within 1–45 days (Russmann *et al.*, 2005). In the patients with FLX-induced liver injury, fever and immune cell infiltration have been observed. This suggests that the pathogenesis of FLX-induced liver injury involves inflammation, but the etiology of FLX-induced liver injury is unknown. 5′-Hydroxymethylflucloxacillin (5′-OH FLX), which is metabolized by CYP3A4, has cytotoxicity in biliary epithelial cells (Lakehal *et al.*, 2001), FLX causes adduct formation in rat liver proteins (Carey and van Pelt, 2005) and FLX and 5′-OH FLX are haptenated with Human Serum Albumin (HSA) *in vivo* and *in vitro*. It was suggested by a genome-wide association study (GWAS) that *HLA-B*57:01* is involved in FLX-induced liver injury (Daly *et al.*, 2009). Dicloxacillin (DCX), which is a semi-synthetic penicillin like FLX, also induces hepatotoxicity (Olsson *et al.*, 1992). We have previously reported that IL-4 mediates DCX-induced liver injury in the mouse (Higuchi *et al.*, 2011). It seems that immune-related factors are also associated with FLX hepatotoxicity.

Recently, immune cells and immune-mediated factors were reported to play critical roles for DILI (Adams *et al.*, 2010). A main contributing factor for DILI is the toll-like receptor (TLR). TLRs are pattern recognition receptors and are expressed in innate immune cells. They release inflammatory cytokines, such as tumor necrosis factor-alpha (TNF-α), interleukin (IL)-1β and IL-6, by ligand binding. TLRs are related to liver diseases, and TLR4 is the most reported to be involved in liver diseases including alcohol-induced hepatitis (Uesugi *et al.*, 2001), hepatic-ischemia

*Correspondence to: Tsuyoshi Yokoi, Drug Metabolism and Toxicology, Faculty of Pharmaceutical Sciences, Kanazawa University, Kakuma-machi, Kanazawa, 920–1192, Japan.
E-mail: tyokoi@med.nagoya-u.ac.jp

[a]Drug Metabolism and Toxicology, Faculty of Pharmaceutical Sciences, Kanazawa University, Kakuma-machi, Kanazawa 920-1192, Japan

[b]Department of Diagnostic Pathology, Graduate School of Medicine and Pharmaceutical Science for Research, University of Toyama, Sugitani, Toyama, 930-0194, Japan

[c]Department of Drug Safety Sciences, Nagoya University Graduate School of Medicine, Tsurumai-cho, Showa-ku, Nagoya, 466-8550, Japan

reperfusion (Tsung *et al.*, 2005), acetaminophen- (Yohe *et al.*, 2006) and halothane-induced liver injury (Dugan *et al.*, 2011).

It is known that some cytokines are involved in DILI. Interferon (IFN)γ, IL-1β, IL-4 and IL-17 are involved in acetaminophen-, diclofenac-, methimazole- and halothane-induced liver injury, respectively (Ishida *et al.*, 2002; Kobayashi *et al.*, 2009, 2012; Yano *et al.*, 2012). These cytokines contribute to immune cell activation, infiltration and cell apoptosis. IL-4 is a Th2-related cytokine and acts to differentiate Th2 cells. IL-17 is a strong inflammatory cytokine that activates neutrophils and is produced by Th17, natural killer (NK) cells, NKT cells and macrophages. Reports have suggested that immune-mediated factors are important for the development of DILI, regardless of cytotoxicity or cholestasis.

The purpose of this study was to establish a mouse model of FLX-induced liver injury and to clarify whether immune- and inflammatory-related factors are associated with FLX hepatotoxicity.

Materials and Methods

Chemicals

FLX was kindly provided by GlaxoSmithKline (London, UK). Ampicillin (AMP), glutathione and 5,5′-dithiobis (2-nitrobenzoic acid) were purchased from Wako (Tokyo, Japan). RNAiso was purchased from Nippon Gene (Tokyo, Japan). ReverTra Ace was obtained from Toyobo (Tokyo, Japan). Random hexamers and SYBR Premix Ex Taq were obtained from Takara (Osaka, Japan). The recombinant mouse IL-17 (rIL-17) and anti-IL-17 antibodies were obtained from R&D Systems (Minneapolis, MN, USA). A high-mobility group box 1(HMGB1) enzyme-linked immunosorbent assay (ELISA) kit and a protein carbonyl assay kit were obtained from Shino-Test (Kanagawa, Japan) and Cayman Chemical (Ann Arbor, MI, USA), respectively. Fuji DRI-CHEM slides of GPT/ALT-PIII and TBIL-PIII used to measure alanine aminotransferase (ALT), aspartate aminotransferase (AST) and total-bilirubin (T-Bil), respectively, were purchased from FujiFilm (Tokyo, Japan). A rabbit polyclonal antibody against myeloperoxidase (MPO) was obtained from DAKO (Carpinteria, CA, USA). All the primers (Table 1) were commercially synthesized at Hokkaido System Sciences (Sapporo, Japan). All other chemicals were of analytical grade or the highest grade commercially available.

Mouse Models of FLX-Induced Liver Injury

Female BALB/cCrSlc mice (6 weeks old) were obtained from SLC Japan (Hamamatsu, Japan). The mice were housed in a controlled

Table 1. Sequences of the primers used for real-time reverse transcription (RT)-PCR analyses

Gene		Sequence	Amplicon size
CXCL1	F (5′-3′)	GAT TCA CCT CAA GAA CAT CCA GAG	221
	R (5′-3′)	GAA GCC AGC GTT CAC CAG AC	
GATA-3	F (5′-3′)	GGA GGA CTT CCC CAA GAG CA	169
	R (5′-3′)	CAT GCT GGA AGG GTG GTG A	
IFN-γ	F (5′-3′)	GGC CAT CAG CAA CAT AAG C	162
	R (5′-3′)	TGG ACC ACT CGG ATG AGC TCA	
IL-1β	F (5′-3′)	GTT GAC GGA CCC CAA AAG AT	277
	R (5′-3′)	CAC ACA CCA GCA GGT TAT CA	
IL-5	F (5′-3′)	AAA GAG ACC TTG ACA CAG CTG	152
	R (5′-3′)	CCA CGG ACA GTT TGA TTC TTC	
IL-6	F (5′-3′)	CCA TAG CTA GGA GTA CA	151
	R (5′-3′)	GGA AAT TGG GGT AGG AAG GA	
MCP-1	F (5′-3′)	TGT CAT GCT TCT GGG CCT G	209
	R (5′-3′)	CCT CTC TCT TGA GCT TGG TG	
MIP-2	F (5′-3′)	AAG TTT GCC TTG ACC CTG AAG	174
	R (5′-3′)	ATC AGG TAC GAT CCA GGC TTC	
ROR-γt	F (5′-3′)	ACC TCC ACT GCC AGC TGT GTG CTG TC	369
	R (5′-3′)	TCA TTT CTG CAC TTC TGC ATG TAG ACT GTC CC	
S100A8	F (5′-3′)	GAG TGT CCT CAG TTT GTG CAG	190
	R (5′-3′)	TAG ACA TAT CCA GGG ACC CAG	
S100A9	F (5′-3′)	GAT GGC CAA CAA AGC ACC TT	236
	R (5′-3′)	CCT CAA AGC TCA GCT GAT TG	
T-bet	F (5′-3′)	CAA GTG GGT GCA GTG TGG AAA G	367
	R (5′-3′)	TGG AGA GAC TGC AGG ACG ATC	
TLR4	F (5′-3′)	TTC TTC TCC TGC CTG ACA CC	251
	R (5′-3′)	CCA TGC CAT GCC TTG TCT TC	
TNF-α	F (5′-3′)	TGT CTC AGC CTC TTC TCA TTC C	142
	R (5′-3′)	TGA GGG TCT GGG CCA TAG AAC	
β-actin	F (5′-3′)	ACG GCC AGG TCA TCA TCA CTA TTG G	238
	R (5′-3′)	CTA GGA GCC AGA GCA GTA ATC TC	

F, forward primer; R, reverse primer; IFN-γ, interferon-γ; IL, interleukin; MIP, macrophage inflammatory protein; MCP, monocyte chemoattractant protein; T-bet, T box expressed in T cells; GATA, GATA-binding protein; ROR, retinoid-related orphan receptor; TNF, tumor necrosis factor.

environment (temperature 25 ± 1 °C, humidity 50 ± 10% and 12-h light/12-h dark cycle) in the institutional animal facility with access to food and water *ad libitum*. The animals were acclimatized before the experiments. The mice were administered FLX (300, 600, 800 and 1000 mg kg^{-1}, dissolved in saline) intraperitoneally (i.p.) in a non-fasting condition. One and a half, three, six, 12 and 24 h after the FLX administration, blood was collected from the inferior vena cava for assessing the ALT, AST T-Bil and HMGB1, and the liver from the largest lobe was used for histopathological examination and the preparation of mRNA. A portion of each excised liver was fixed in a 10% formalin neutral buffer solution and used for immunohistochemical staining. The degree of liver injury was assessed by hematoxylin-eosin (H&E) staining. The infiltration of mononuclear cells was assessed by immunostaining for MPO. A rabbit polyclonal antibody against MPO was used for immunohistochemical staining of the liver as previously described (Kumada *et al.*, 2004). Animal maintenance and treatments were conducted in accordance with the National Institutes of Health Guide for Animal Welfare of Japan, as approved by the Institutional Animal Care and Use Committee of Kanazawa University, Japan.

Real-Time Reverse Transcription (RT)-PCR

RNA from the mouse livers was isolated using RNAiso according to the manufacturer's instructions. CXC kemokine-ligand-1 (CXCL1), GATA-binding protein (GATA)-3, IFN-γ, IL-1β, IL-5, IL-6, monocyte chemoattractant protein (MCP)-1, macrophage inflammatory protein (MIP)-2, retinoid-related orphan receptor (ROR)-γt, S100A8, S100A9, T box expressed in T cells (T-bet), TLR4, TNFα and β-actin were quantified by real-time RT-PCR. The primer sequences used in this study are shown in Table 1. For the RT-process, total RNA (10 μg) and 150 ng of random hexamers were mixed and incubated at 70 °C for 10 min. The RNA solution was added to a reaction mixture containing 100 units of ReverTra Ace, reaction buffer and 0.5 mM dNTPs in a final volume of 40 μl. The reaction mixture was incubated at 30 °C for 10 min, 42 °C for 1 h and heated at 98 °C for 10 min to inactivate the enzyme. The real-time RT-PCR contained 1 or 2 μl of the template cDNA, SYBR Premix Ex Taq solution and 8 pmol of the forward and reverse primers. The amplified products were monitored directly by measuring the increase in the dye intensity of the SYBR Green I (Molecular Probes, Eugene, OR, USA) binding to the double-stranded DNA amplified by the PCR. Melting curve analysis and agarose gel electrophoresis were performed to confirm a single PCR product with the correct amplicon length.

Administration of Recombinant Mouse IL-17 (rIL-17) or Anti-Mouse IL-17 Antibodies

One hour after FLX administration, rIL-17 was i.p. administered [2.0 μg of rIL-17 in 0.2 ml of sterile phosphate-buffered saline (PBS) containing 0.5% bovine serum albumin] in a non-fasting condition. In the neutralization study, the mice were given an anti-mouse IL-17 antibody i.p. (100 μg of anti-mouse IL-17 antibody in 0.2 ml of sterile PBS) 1 h before the flucloxacillin administration. As a control, rat IgG2a was given (100 μg of rat IgG2a in 0.2 ml of sterile PBS).

Measurement of Plasma HMGB1 Level

The plasma HMGB1 level was measured by ELISA using a HMGB1 ELISA Kit II. Sample diluent 100 μl was added to each well. A 10-μl sample was added to each well and incubated for 24 h at 37 °C. After washing the wells five times, 100 μl of the peroxidase-conjugate solution was added to each well and incubated at 25 °C for 2 h. After washing the wells five times, 100 μl of the substrate solution was added to each well and incubated at room temperature for 30 min. The stop solution (100 μl) was added, and the absorbance at 450 nm was measured.

Glutathione Content and Protein Carbonyl Assay

The mouse liver tissue was homogenized with a glass homogenizer on ice-cold 5% sulfosalicylic acid and centrifuged at 8000 *g* at 4 °C for 10 min. The total GSH (the sum of the reduced and oxidized forms) was measured using reduced GSH as a standard. The supernatant was diluted with distilled water, and the GSH concentration was measured as described previously (Griffith, 1980). The GSH standard curve (0.035–0.55 μmol g^{-1} protein) showed good linearity ($R > 0.99$).

Protein carbonyl was measured using a protein carbonyl assay kit. 2,4-Dinitrophenylhydrazine (800 μl) was added to a 200-μl sample. The samples were incubated in the dark at room temperature for 1 h and vortexed briefly every 15 min during the incubation. One milliliter of 20% TCA was added, vortexed and incubated for 5 min. After centrifugation at 10 000 *g* for 10 min at 4 °C, the supernatant was discarded, and the pellet was resuspended and centrifuged at 10 000 *g* at 4 °C for 10 min two times. The protein pellets were resuspended in 500 μl of guanidine hydrochloride and centrifuged at 10 000 *g* at 4 °C for 10 min. The absorbance at a wavelength between 360–385 nm was measured.

Statistical Analysis

The data are presented as the mean ± SEM. Statistical analyses between multiple groups were performed using one-way analysis of variance (ANOVA), followed by Tukey's *post hoc* test, and comparisons between two groups were carried out using a two-tailed Student's *t*-test for the mRNA and plasma HMGB1 levels. For the ALT and T-Bil levels, a non-parametric statistical analysis was conducted using the Mann–Whitney *U*-test and the Kruskal–Wallis test. $^*P < 0.05$ was considered statistically significant.

Results

Increase in the Plasma ALT, AST and T-Bil levels in FLX-Administered Mice

To investigate dose-dependent changes in the plasma ALT and AST, female BALB/c mice were administered FLX at doses of 300, 600, 800 and 1000 mg kg^{-1}. Six hours after the administration, the plasma ALT and AST showed dose-dependent increases and were significantly increased at doses of 800 and 1000 mg kg^{-1} of FLX compared with the control (Fig. 1A). To investigate time-dependent changes in the plasma ALT, AST and T-Bil, mice were administered FLX at a dose of 1000 mg kg^{-1}. The plasma ALT, AST and T-Bil were significantly

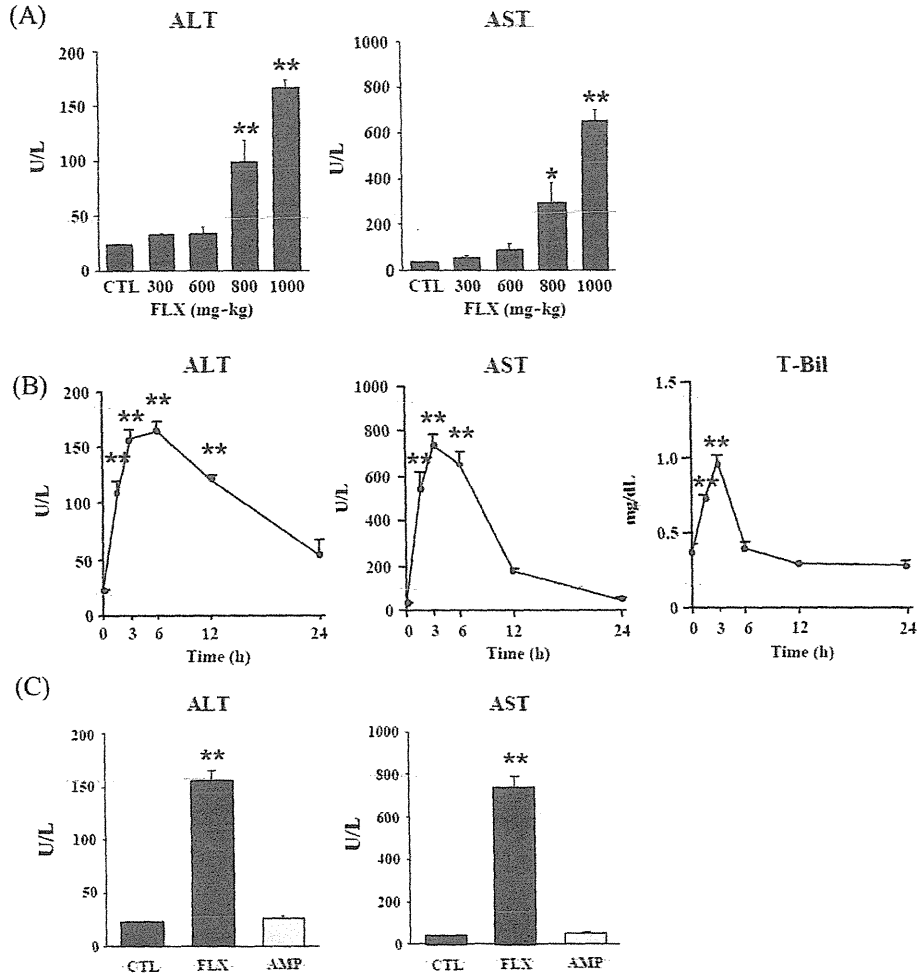

Figure 1. Dose- and time-dependent changes in plasma biomarkers in flucloxacillin (FLX)-administered mice. (A) Mice were administered FLX [300, 600, 800 and 1000 mg kg^{-1}, intraperitoneally (i.p.)]. Six hours after the administration, the plasma, alanine aminotransferase (ALT) and aspartate aminotransferase (AST) levels were measured. (B) The plasma ALT, AST and total bilirubin (T-Bil) levels were measured 1.5, 3, 6, 12 and 24 hafter administration of FLX (1000 mg kg^{-1}, i.p.). (C) Mice were administered FLX (1000 mg kg^{-1}, i.p.) or ampicillin (AMP) (1000 mg kg^{-1}, i.p.). Three hours after the administration, the plasma ALT and AST levels were measured. The data are shown as the mean ± SEM of the results from four to six mice. The differences compared with the control mice (A), (C), or with the time before the administration (B) were considered significant at $^{*}P < 0.05$ and $^{**}P < 0.01$.

increased at 1.5, 3, 6 and 12 h, 1.5, 3 and 6 h, and 1.5 and 3 h, respectively, after FLX administration (Fig. 1B). To investigate the impact of the pharmacological effect on FLX-induced liver injury, we used AMP, which is a β-lactam antibiotic with much less hepatotoxicity and similar pharmacological properties and chemical structure to FLX. The administration of AMP did not result in an increase in the plasma ALT or AST (Fig. 1C).

Expression of TLR4 Ligands in FLX-Induced Liver Injury

To investigate the involvement of TLR4 in FLX-induced hepatotoxicity, the hepatic mRNA levels of S100A8 and S100A9 and the plasma HMGB1 level were measured by real-time RT-PCR and ELISA, respectively. HMGB1 is released from necrotic cells or activated immune cells, and S100A8 and S100A9 are localized in the cytoplasm and/or nucleus of a wide range of cells and are released by phagocytes. HMGB1, S100A8 and S100A9 are ligands of TLR4 expressed in immune-related cells. They activate downstream signaling pathway of TLR4, and then induce inflammatory factors such as IL-1β and TNFα. Thus, the activation of TLR4 by those ligands is necessary to develop inflammation. As the results, the hepatic mRNA levels of S100A8 and S100A9 were significantly increased at 3 h, 1.5 and 3 h, respectively, after the administration of FLX compared with the non-treated controls (Fig. 2A). The plasma HMGB1 level was significantly increased at 1.5 and 3 h (Fig. 2B). These changes suggested the involvement of a TLR4-associated signal cascade.

Time-Dependent Changes in the mRNA Expression of Inflammatory-Related Factors in FLX-Induced Liver Injury

To investigate if inflammatory-related factors are involved in FLX-induced liver injury, the hepatic mRNA levels of IL-1β, TNFα, MCP-1, MIP-2 and CXCL1 were measured by real-time RT-PCR. The hepatic mRNA levels of IL-1β, TNFα, MCP-1, MIP-2 and CXCL1 were significantly increased at 3 and 6 h, 6 h, 3 and 12 h, 1.5 and

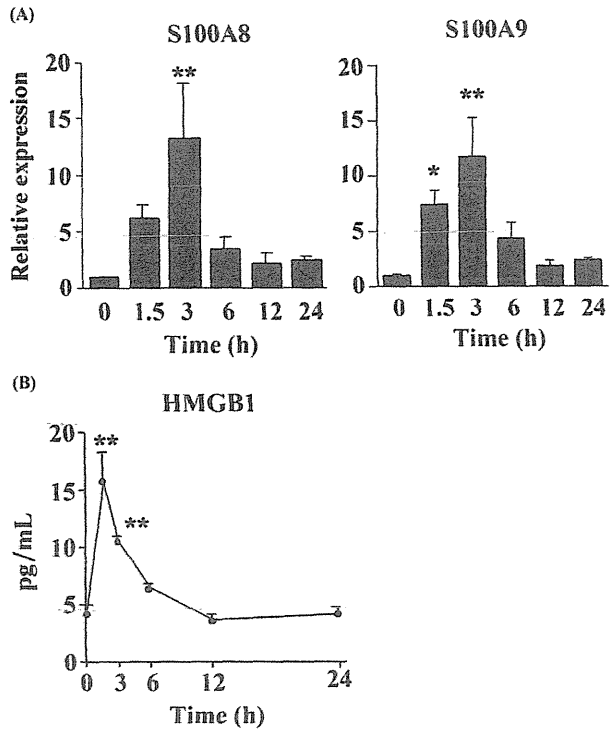

Figure 2. Time-dependent changes in the hepatic expression levels of S100A8 and S100A9 mRNA and the plasma HMGB1 level in flucloxacillin (FLX)-administered mice. (A) The expression levels of hepatic S100A8 and S100A9 mRNA levels were measured by real-time RT-PCR 1.5, 3, 6, 12 or 24 h after administration of FLX [1000 mg kg^{-1}, intraperitoneally (i.p.)]. The expression level of hepatic mRNA was normalized to that of β-actin mRNA. (B) The plasma HMGB1 protein levels were measured by enzyme-linked immunosorbent assay (ELISA). The data are shown as the mean ± SEM of the results from four to six mice. The differences compared with the control mice were considered significant at $^{*}P < 0.05$ and $^{**}P < 0.01$.

3 h, 1.5 and 3 h, respectively in the FLX-induced liver injury mice compared with the non-treated controls. This suggests that these inflammatory-related factors might be involved in the FLX-induced liver injury (Fig. 3).

Time-Dependent Changes in the mRNA Expression of Immune-Related Transcriptional Factors and Cytokines in FLX-Induced Liver Injury

To investigate the contribution of immune-related transcriptional factors and cytokines to FLX-induced liver injury, the expression of the hepatic mRNA of T-bet, GATA-3, IFN-γ, IL-5 and IL-6 were measured by real-time RT-PCR. The expression levels of T-bet were significantly decreased at 1.5 to 12 h after the FLX administration compared with the non-treated controls. The expression levels of IFN-γ and GATA-3 were unchanged. The expression levels of ROR-γt, IL-5 and IL-6 were significantly increased at 3 and 12 h, 1.5 h, 1.5 and 3 h, respectively, after the administration of FLX compared with the non-treated controls (Fig. 4). It is known that IFNγ and GATA-3 are the representative factor of Th1 and Th2 cells, respectively. Thus, it was suggested that IFNγ and GATA-3 were not involved in FLX-induced liver injury (Fig. 4). ROR-γt is a transcription factor of NK cells, NKT cells and Th17 cells. IL-6 is a pleiotropic cytokine involved in the enhancing expression and activation of IL-17. The mRNA expression levels of ROR-γt and IL-6 were significantly increased (Fig. 4), therefore we thought that IL-17 is involved in FLX-induced liver injury.

Effect of rIL-17 and anti-IL-17 Antibody Administration in FLX-Induced Liver Injury

To investigate if IL-17 is involved in FLX-induced liver injury, FLX was co-administered with rIL-17 (2 mg/body, i.p.). The plasma ALT was significantly increased, and the plasma AST showed a tendency to increase in the mice co-administered FLX and rIL-17 (Fig. 5A) compared with the FLX-administered mice. In the histopathological examinations of the liver, immune cell infiltration and necrotic cells were observed in the mice administered FLX and rIL-17 by hematoxylin-eosin staining (Fig. 5B). In the immunohistochemical analysis, the numbers of MPO-positive cells were significantly increased in the mice administered FLX and rIL-17 (Fig. 5C) compared with the FLX-administered mice. In a neutralization study, 1 h before the administration of FLX, the mice were administered an anti-IL-17 antibody. At 3 h after the administration of FLX, the plasma ALT and AST levels showed a tendency to decrease compared with the FLX-administered mice (Fig. 5D).

Involvement of GSH and Oxidative Stress in FLX-Induced Liver Injury

The hepatic GSH content was significantly decreased at 1.5 and 3 h in the FLX-administered mice compared with the non-treated mice. The GSSG level was significantly increased at 1.5 and 6 h after the administration of FLX compared with the non-treated controls. The GSH/GSSG ratio, which is used as an oxidative stress marker, exhibited a similar profile to that obtained for the GSH level (Fig. 6A). The protein carbonyl levels were not significantly changed compared with the non-treated controls (Fig. 6B).

Discussion

In this study, we established a mouse model of FLX-induced liver injury and suggested that immune- and inflammatory-related factors are involved in the hepatotoxicity of FLX. Many clinical case reports of FLX-induced liver injury have been published since 1982 (Olsson *et al.*, 1992), but the mechanism of FLX-induced liver injury has not been fully elucidated. This is the first report to clarify the mechanism of FLX-induced liver injury using a mouse model.

The administration of FLX in mice resulted in an increase in the plasma ALT, AST and T-Bil levels. The plasma AST level was more elevated than the plasma ALT level (Fig. 1A and B), which is similar to the results of a clinical case report (Törnhage *et al.*, 2009). The elevation of the plasma T-Bil level in the mouse was similar to that in humans because jaundice was observed in 95% of patients with FLX-induced liver injury (Devereaux *et al.*, 1995). To investigate if the pharmacological effect of FLX has an effect on the liver injury, AMP, which has similar pharmacological properties and chemical structure to those of FLX and has been reported to be much less hepatotoxic than FLX (Andrade & Tulkens, 2011), was administered to mice (Fig. 1C). The results showed that the pharmacological effect was not involved in the FLX-induced liver injury.

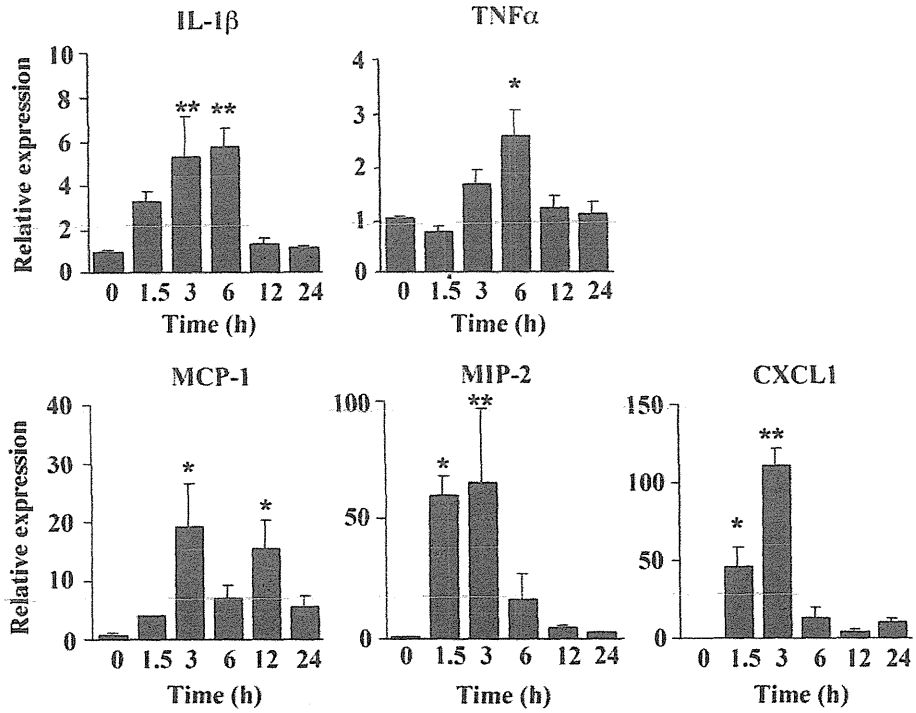

Figure 3. Time-dependent changes in the hepatic mRNA expression levels of inflammatory-related factors in flucloxacillin (FLX)-administered mice. The expression levels of hepatic mRNA were measured by real-time reverse transcription (RT)-PCR 1.5, 3, 6, 12 or 24 h after the FLX administration [1000 mg kg^{-1}, intraperitoneally (i.p.)]. The expression level of hepatic mRNA was normalized to that of β-actin mRNA. The data are shown as the mean ± SEM of the results from four to six mice. The differences compared with the control mice were considered significant at $^{*}P < 0.05$ and $^{**}P < 0.01$.

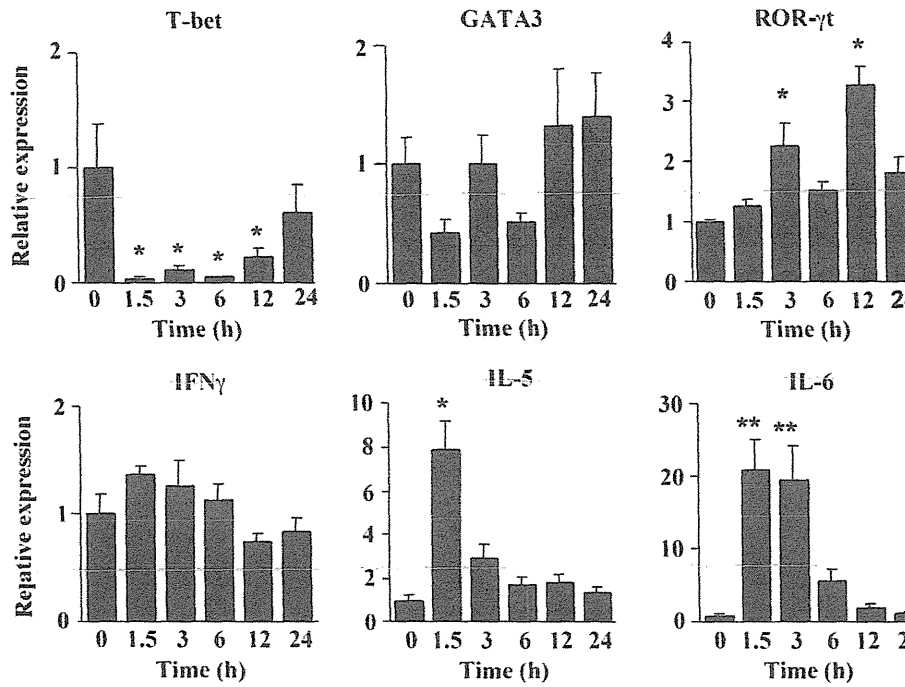

Figure 4. Time-dependent changes in the hepatic expression levels of transcriptional factors and cytokines in flucloxacillin (FLX)-administered mice. The hepatic mRNA levels were measured by real-time reverse transcription (RT)-PCR 1.5, 3, 6, 12 or 24 h after the administration of FLX [1000 mg kg^{-1}, intraperitoneally (i.p.)]. The expression level of hepatic mRNA was normalized to that of β-actin mRNA. The data are shown as the mean ± SEM of the results from four to six mice. The differences compared with the control mice were considered significant at $^{*}P < 0.05$ and $^{**}P < 0.01$.

Journal of AppliedToxicology

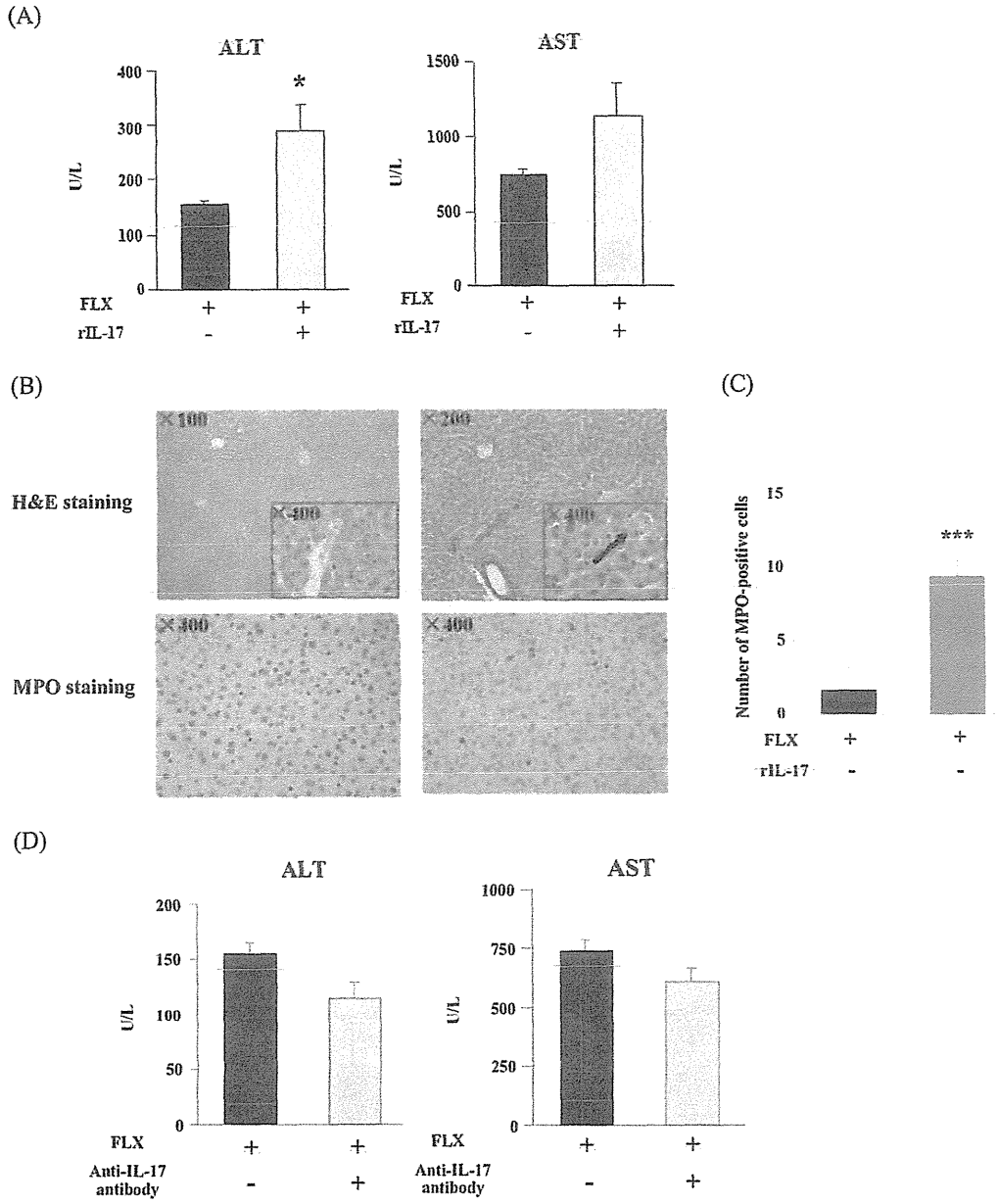

Figure 5. Involvement of interleukin (IL)-17 in flucloxacillin (FLX)-induced liver injury in mice. (A) One hour after the administration of FLX [1000 mg kg^{-1}, intraperitoneally (i.p.)], rIL-17 (2 μg per body weight, i.p.) was administered. Three hours after the administration of FLX, the plasma alanine aminotransferase (ALT) and aspartate aminotransferase (AST) levels were measured. (B) Liver sections from the FLX (1000 mg kg^{-1}, i.p.)-administered mice were stained with hematoxylin and eosin (H&E) or immunostained with an anti-myeloperoxidase (MPO) antibody. A green arrow indicates an immune cell infiltration, and a black arrow indicates a necrotic cell. (C) The number of MPO-positive cells was compared with those in mice given FLX. (D) One hour before FLX (1000 mg kg^{-1}, i.p.) administration, an anti-IL-17 antibody (100 μg body weight, i.p.) was administered. Three hours after the administration of FLX, the plasma ALT and AST levels were measured. The data are shown as the mean ± SEM of the results from four. The differences compared with the control mice were considered significant at $^{*}P < 0.05$ and $^{***}P < 0.001$.

TLR4 was first recognized as a receptor for host defenses. TLR4 is involved in many diseases, and its endogenous ligands such as S100A8/A9 and HMGB1 have been identified. S100A8 and S100A9 are released from activated phagocytes, and they are associated with inflammation and cancer (Gebhardt *et al.*, 2006; Foell *et al.*, 2007). S100A8 and S100A9 are also increased in the plasma by TLR4 activation (Boyd *et al.*, 2008; Ehrchen *et al.*, 2009). HMGB1 is released from necrotic cells and activated immune cells and binds TLR4 to promote the production of inflammatory cytokines (Sims *et al.*, 2010). It has been reported that HMGB1 is responsible for hepatic ischemia and reperfusion and acetaminophen- and halothane-induced liver injury (Tsung *et al.*, 2005; Antoine *et al.*, 2009; Dugan *et al.*, 2011). We investigated the expression changes of S100A8, S100A9 and HMGB1. The maximum level of HMGB1 was demonstrated 1.5 h after the administration of FLX, which is earlier than that of the plasma ALT, AST, S100A8 and S100A9 (Fig. 2A and B). Considering from these data, we thought that the mechanism is as follows: (1) inflammatory-related cells were activated by FLX or its metabolite(s) in the liver; (2) the released HMGB1

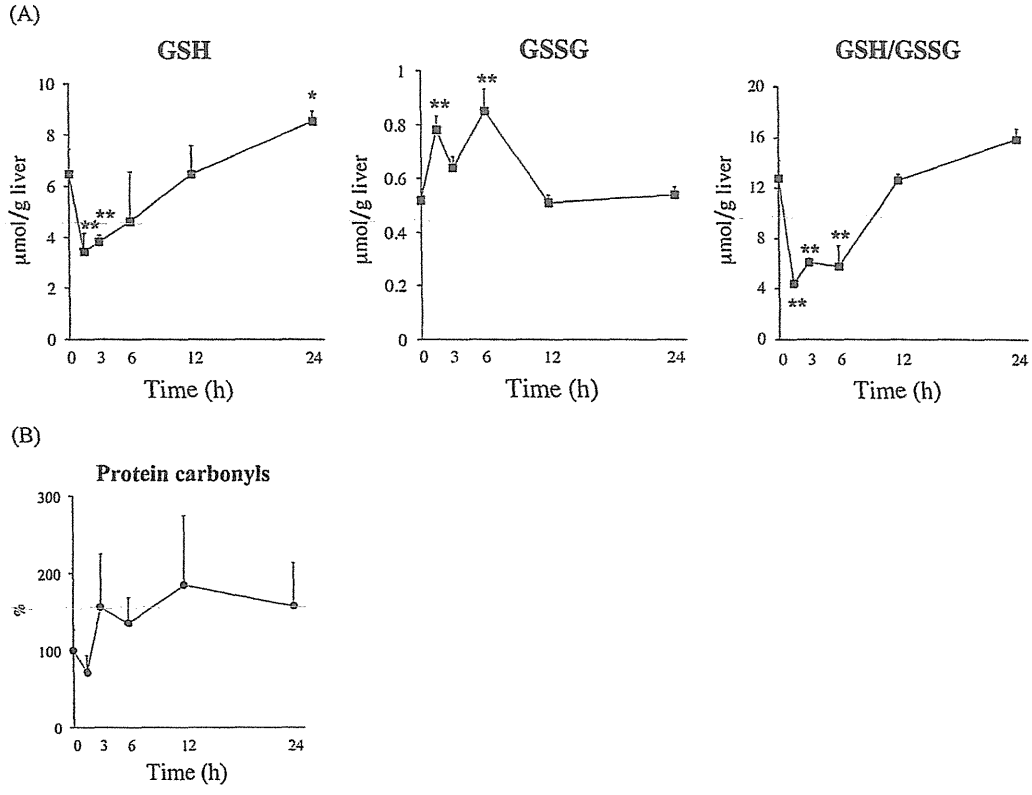

Figure 6. Time-dependent changes in the hepatic GSH and GSSG levels and GSH/GSSG ratio and the levels of protein carbonyls in flucloxacillin (FLX)-administered mice. (A) The content of GSH, GSSG and (B) protein carbonyl were measured in the liver tissue homogenate. The data are shown as the mean ± SEM of the results from four to six mice. The differences compared with the control mice were considered significant at $^{*}P < 0.05$ and $^{**}P < 0.01$.

binds to TLR4 in macrophages; and (3) the production of S100A8, S100A9 and inflammatory factors was increased by the activated TLR4.

To further investigate if TLR4 promoted inflammation in FLX-induced liver injury, we measured the expression levels of IL-1β, TNFα, MCP-1, MIP-2 and CXCL1 mRNA produced by the activation of TLR4 (Asehnoune *et al.*, 2004; De Filippo *et al.*, 2008; Li *et al.*, 2011). The expression levels of these proteins were reported to be increased when the mRNAs are elevated (Sass *et al.*, 2002; Roche *et al.*, 2008; Imaeda *et al.*, 2009). IL-1β has roles in inflammation and the activation of immune cells (Dinarello, 2011). TNF-α is associated with cell apoptosis (Malhi *et al.*, 2006). MCP-1, MIP-2 and CXCL1 attract immune cells in tissues (Adams *et al.*, 2010). These proteins are involved in immune cell-associated inflammation and cell death. TLR4 activation may lead to the production of inflammatory factors and immune cell activation in FLX-induced liver injury.

It is known that IFNγ, IL-4 and IL-17 are exacerbation factors in liver injury *via* T cell-related immune reactions. The expression of IL-4 was not detected in the present study (data not shown). The expression level of IL-4 is known to correlate with that of GATA-3, demonstrating no changes as shown in Fig. 4. IFNγ and GATA-3 are the representative factor for Th1 and Th2 cells, respectively (Ranganath *et al.*, 1998), thus, it was suggested that IFNγ and GATA-3 were not involved in FLX-induced liver injury.

The plasma IL-17 level showed a low threshold level in the present study (data not shown). ROR-γt is a transcription factor of NK cells, NKT cells and Th17 cells. IL-6 is a pleiotropic cytokine involved in the enhancing expression and activation of IL-17. The mRNA expression levels of ROR-γt and IL-6 were significantly increased (Fig. 4), therefore we thought that IL-17 might be involved in FLX-induced liver injury.

We investigated the effect of rIL-17 and anti-IL-17 antibodies. The plasma ALT was elevated by the co-administration of rIL-17 and FLX, and liver injury was confirmed by histopathology (Fig. 5A and 5B). Previously, we reported that administration of anti-mouse IL-17 antibody (100 μg per mouse) significantly attenuated α-naphthylisothiocyanate-, carbamazepine-, halothane- and phenytoin-induced liver injury in mice (Kobayashi *et al.*, 2009; Kobayashi *et al.*, 2010; Higuchi *et al.*, 2012; Sasaki *et al.*, 2013). IL-17 had been identified as involved in thee drug-induced liver injury. Therefore, we conducted the same method to neutralize IL-17 in the present study, suggesting the involvement of IL-17 in FLX-induced liver injury (Fig. 5D). Taking these results into consideration, IL-17 would be an exacerbating factor, but its contribution to DILI might not be strong.

GSH is known to have two functions: the antioxidant regent by forming GSSG and the conjugated substrate of reactive metabolites. Therefore, we measured the cellular GSH content to determine which has the major role. We considered that oxidative stress had a limited effect on FLX-induced liver injury, because protein carbonyl, an oxidative biomarker, did not change significantly (Fig. 6B). It has been suggested that the parent compound of FLX has no or much less toxicity, but 5′–OH FLX induced cytotoxicity in culture of human hepatocytes and biliary epithelial cells (Lakehal *et al.*, 2001). However, GSH conjugation of FLX metabolite(s) *in vivo* has never been reported. It has been reported

that penicillin derivatives are metabolized to penicillanic acid and penicilloic acid, which are sulfur-containing compounds and bind to protein (Stachulski *et al.*, 2013). GSH has the ability to bind sulfur-containing groups such as the thiol group. Thus, we thought GSH conjugates the sulfur-containing group of FLX-metabolites. In the present study, GSH and the GSH/GSSG ratio decreased until 6 h after the administration of FLX, and the protein carbonyl levels showed no significant changes (Fig. 6A and B). These results suggest that GSH might conjugate reactive metabolite(s) of FLX, but the contribution of reactive metabolite(s) for DILI might be limited.

In our previous study, DCX-induced liver injury was exacerbated by IL-4 (Higuchi *et al.*, 2011), but it was unclear why the exacerbation factors were different for FLX and DCX. There is only one atom difference of fluorine (F) and chloride (Cl) at position 6 of phenyl group. Olsson *et al.* (1992) reported that the patients who developed FLX-induced liver injury did not have detectable antibodies, but approximately half of the patients who developed DCX-induced liver injury had detectable antibodies. The differences in the atomic radius and electronegativity between F and Cl affect the responses of the immune cells.

An HLA association with the *HLA-B*57:01* allele has been reported in FLX-induced liver injury in humans (Daly *et al.*, 2009; Wuillemin *et al.*, 2013). The involvement of activated T cells in the immune pathomechanism of liver damage has been suggested (Monshi *et al.*, 2013). This study will provide useful information to clarify the detailed immune pathomechanism of FLX-induced liver injury.

This study showed that immune- and inflammatory-related factors are involved in the pathogenesis and exacerbation of FLX-induced liver injury. The TLR4 signaling cascade was suggested to be associated with the etiology, and IL-17 might be an exacerbating factors. This study might provide beneficial information about FLX-induced liver injury and similar drug-induced hepatotoxicities.

Funding

This study was supported by Health and Labor Sciences Research Grants from the Ministry of Health, Labor and Welfare of Japan (H23-BIO-G001)

Conflict of Interest

The Authors did not report any conflict of interest.

References

Adams DH, Ju C, Ramaiah SK, Uetrecht J, Jaeschke H. 2010. Mechanisms of immune-mediated liver injury. *Toxicol. Sci.* **115**: 307–321.

Andrade RJ, Tulkens PM. 2011. Hepatic safety of antibiotics used in primary care. *J. Antimicrob. Chemother.* **66**: 1431–1446.

Antoine DJ, Williams DP, Kipar A, Jenkins RE, Regan SL, Sathish JG, Kitteringham NR, Park BK. 2009. High-mobility group box-1 protein and keratin-18, circulating serum proteins informative of acetaminophen-induced necrosis and apoptosis *in vivo*. *Toxicol. Sci.* **112**: 521–531.

Asehnoune K, Strassheim D, Mitra S, Kim JY, Abraham E. 2004. Involvement of reactive oxygen species in Toll-like receptor 4-dependent activation of NF-kappa B. *J. Immunol.* **172**: 2522–2529.

Björnsson E, Olsson R. 2005. Outcome and prognostic markers in severe drug-induced liver disease. *Hepatology* **42**: 481–489.

Boyd JH, Kan B, Roberts H, Wang Y, Walley KR. 2008. S100A8 and S100A9 mediate endotoxin-induced cardiomyocyte dysfunction *via* the receptor for advanced glycation end products. *Circ. Res.* **23**: 1239–1246.

Carey MA, van Pelt FN. 2005. Immunochemical detection of flucloxacillin adduct formation in livers of treated rats. *Toxicology* **216**: 41–48.

Daly AK, Donaldson PT, Bhatnagar P, Shen Y, Pe'er I, Floratos A, Daly MJ, Goldstein DB, John S, Nelson MR, Graham J, Park BK, Dillon JF, Bernal W, Cordell HJ, Pirmohamed M, Aithal GP, Day CP. 2009. HLA-B*5701 genotype is a major determinant of drug-induced liver injury due to flucloxacillin. *Nat. Genet.* **41**, 816–819.

De Filippo K, Henderson RB, Laschinger M, Hogg N. 2008. Neutrophil chemokines KC and macrophage-inflammatory protein-2 are newly synthesized by tissue macrophages using distinct TLR signaling pathways. *J. Immunol.* **180**: 4308–4315.

Devereaux BM, Crawford DH, Purcell P, Powell LW, Roeser HP, 1995. Flucloxacillin associated cholestatic hepatitis. An Australian and Swedish epidemic? *Eur. J. Clin. Pharmacol.* **49**: 81–85.

Dinarello CA. 2011. A clinical perspective of IL-1β as the gatekeeper of inflammation. *Eur. J. Immunol.* **41**: 1203–1217.

Dugan CM, Fullerton AM, Roth RA, Ganey PE. 2011. Natural killer cells mediate severe liver injury in a murine model of halothane hepatitis. *Toxicol. Sci.* **120**: 507–518.

Ehrchen JM, Sunderkötter C, Foell D, Vogl T, Roth J. 2009. The endogenous Toll-like receptor 4 agonist S100A8/S100A9 (calprotectin) as innate amplifier of infection, autoimmunity, and cancer. *J. Leukoc. Biol.* **86**: 557–566.

Foell D, Wittkowski H, Vogl T, Roth J. 2007. S100 proteins expressed in phagocytes: a novel group of damage-associated molecular pattern molecules. *J. Leukoc. Biol.* **81**: 28–37.

Gebhardt C, Németh J, Angel P, Hess J. 2006. S100A8 and S100A9 in inflammation and cancer. *Biochem. Pharmacol.* **72**: 1622–1631.

Griffith OW. 1980. Determination of glutathione and glutathione disulfide using glutathione reductase and 2-vinylpyridine. *Anal. Biochem.* **106**: 207–212.

Higuchi S, Kobayashi M, Yoshikawa Y, Tsuneyama K, Fukami T, Nakajima M, Yokoi T. 2011. IL-4 mediates dicloxacillin-induced liver injury in mice. *Toxicol. Lett.* **200**: 139–145.

Higuchi S, Yano A, Takai S, Tsuneyama K, Fukami T, Nakajima M, Yokoi T. 2012. Metabolic activation and inflammation reactions involved in carbamazepine-induced liver injury. *Toxicol. Sci.* **130**: 4–16.

Ishida Y, Kondo T, Ohshima T, Fujiwara H, Iwakura Y, Mukaida N. 2002. A pivotal involvement of IFN-g in the pathogenesis of acetaminophen-induced acute liver injury. *FASEB J.* **16**: 1227–1236.

Imaeda AB, Watanabe A, Sohail MA, Mahmood S, Mohamadnejad M, Sutterwala FS, Flavell RA, Mehal WZ. 2009. Acetaminophen-induced hepatotoxicity in mice is dependent on Tlr9 and the Nalp3 inflammasome. *J. Clin. Invest.* **119**: 305–314.

Kaplowitz N. 2005. Idiosyncratic drug hepatotoxicity. *Nat. Rev. Drug Discov.* **4**: 489–499.

Kobayashi E, Kobayashi M, Tsuneyama K, Fukami T, Nakajima M, Yokoi T. 2009. Halothane-induced liver injury is mediated by interleukin-17 in mice. *Toxicol. Sci.* **111**: 302–310.

Kobayashi M, Higuchi S, Mizuno K, Tsuneyama K, Fukami T, Nakajima M, Yokoi T. 2010. Interleukin-17 is involved in alpha-naphthylisothiocyanate-induced liver injury in mice. *Toxicology* **275**: 50–57.

Kobayashi M, Higuchi S, Ide M, Nishikawa S, Fukami T, Nakajima M, Yokoi T. 2012. Th2 cytokine-mediated methimazole-induced acute liver injury in mice. *J. Appl. Toxicol.* **32**: 823–833.

Kumada T, Tsuneyama K, Hatta H, Ishizawa S, Takano Y. 2004. Improved 1-h rapid immunostaining method using intermittent microwave irradiation: practicability based on 5 years application in Toyama Medical and Pharmaceutical University Hospital. *Mod. Pathol.* **17**: 1141–1149.

Lakehal F, Dansette PM, Becquemont L, Lasnier E, Delelo R, Balladur P, Poupon R, Beaune PH, Housset C. 2001. Indirect cytotoxicity of flucloxacillin toward human biliary epitheliumvia metabolite formation in hepatocytes. *Chem. Res. Toxicol.* **14**: 694–701.

Li L, Chen L, Hu L, Liu Y, Sun HY, Tang J, Hou YJ, Chang YX, Tu QQ, Feng GS, Shen F, Wu MC, Wang HY. 2011. Nuclear factor high-mobility group box1 mediating the activation of Toll-like receptor 4 signaling in hepatocytes in the early stage of nonalcoholic fatty liver disease in mice. *Hepatology* **54**: 1620–1630.

Malhi H, Gores GJ, Lemasters JJ. 2006. Apoptosis and necrosis in the liver: a tale of two deaths? *Hepatology* **43**: 31–44.

Monshi MM, Faulkner L, Gibson A, Jenkins RE, Farrell J, Earnshaw CJ, Alfirevic A, Cederbrant K, Daly AK, French N, Pirmohamed M, Park BK, Naisbitt DJ. 2013. Human leukocyte antigen (HLA)-B*57:01-restricted activation of drug-specific T cells provides the immunological basis for flucloxacillin-induced liver injury. *Hepatology* **57**: 727–739.

Olsson R, Wiholm BE, Sand C, Zettergren L, Hultcrantz R, Myrhed M. 1992. Liver damage from flucloxacillin, cloxacillin and dicloxacillin. *J. Hepatol.* **15**: 154–161.

Ranganath S, Ouyang W, Bhattarcharya D, Sha WC, Grupe A, Peltz G, Murphy KM. 1998. GATA-3-dependent enhancer activity in IL-4 gene regulation. *J. Immunol.* **161**: 3822–3826.

Roche JK, Stone MK, Gross LK, Lindner M, Seaner R, Pincus SH, Obrig TG. 2008. Post-exposure targeting of specific epitopes on ricin toxin abrogates toxin-induced hypoglycemia, hepatic injury, and lethality in a mouse model. *Lab. Invest.* **88**: 1178–1191.

Russmann S, Kaye JA, Jick SS, Jick H. 2005. Risk of cholestatic liver disease associated with flucloxacillin and flucloxacillin prescribing habits in the UK: cohort study using data from the UK General Practice Research Database. *Br. J. Clin. Pharmacol.* **60**: 76–82.

Sasaki E, Matsuo K, Iida A, Tsuneyama K, Fukami T, Nakajima M, Yokoi T. 2013. A novel mouse model for phenytoin-induced liver injury: involvement of immune-related factors and P450-mediated metabolism. *Toxicol. Sci.* **136**: 250–263.

Sass G, Heinlein S, Agli A, Bang R, Schümann J, Tiegs G. 2002. Cytokine expression in three mouse models of experimental hepatitis. *Cytokine* **19**: 115–120.

Sims GP, Rowe DC, Rietdijk ST, Herbst R, Coyle AJ. 2010. HMGB1 and RAGE in inflammation and cancer. *Annu. Rev. Immunol.* **28**: 367–388.

Stachulski AV, Baillie TA, Park BK, Obach RS, Dalvie DK, Williams DP, Srivastava A, Regan SL, Antoine DJ, Goldring CE, Chia AJ, Kitteringham NR, Randle LE, Callan H, Castrejon JL, Farrell J, Naisbitt DJ, Lennard MS. 2013. The generation, detection, and effects of reactive drug metabolites. *Med. Res. Rev.* **33**: 985–1080.

Törnhage CJ, Brunlöf G, Wallerstedt SM. 2009. Severe hepatotoxic adverse reaction in a healthy schoolgirl after treatment with flucloxacillin. *Drug Healthc. Patient Saf.* **1**: 17–19.

Tsung A, Sahai R, Tanaka H, Nakao A, Fink MP, Lotze MT, Yang H, Li J, Tracey KJ, Geller DA, Billiar TR. 2005. The nuclear factor HMGB1 mediates hepatic injury after murine liver ischemia-reperfusion. *J. Exp. Med.* **201**: 1135–1143.

Uesugi T, Froh M, Arteel GE, Bradford BU, Thurman RG. 2001. Toll-like receptor 4 is involved in the mechanism of early alcohol-induced liver injury in mice. *Hepatology* **34**: 101–108.

Verma S, Kaplowitz N. 2009. Diagnosis, management and prevention of drug-induced liver injury. *Gut* **58**: 1555–1564.

Wuillemin N, Asam J, Fontana S, Krähenbühl S, Pichler WJ, Yerly D. 2013. HLA haplotype determines hapten or p-I T cell reactivity to flucloxacillin. *J. Immunol.* **190**: 4956–4964.

Yano A, Higuchi S, Tsuneyama K, Fukami T, Nakajima M, Yokoi T. 2012. Involvement of immune-related factors in diclofenac-induced acute liver injury in mice. *Toxicology* **293**: 107–114.

Yohe HC, O'Hara KA, Hunt JA, Kitzmiller TJ, Wood SG, Bement JL, Bement WJ, Szakacs JG, Wrighton SA, Jacobs JM, Kostrubsky V, Sinclair PR, Sinclair JF. 2006. Involvement of Toll-like receptor 4 in acetaminophen hepatotoxicity. *Am. J. Physiol. Gastrointest. Liver Physiol.* **290**: 1269–1279.

Toxicology 319 (2014) 75–84

Contents lists available at ScienceDirect

Toxicology

journal homepage: www.elsevier.com/locate/toxicol

Involvement of miRNAs in the early phase of halothane-induced liver injury

Shinya Endo[a], Azusa Yano[a], Tatsuki Fukami[a], Miki Nakajima[a], Tsuyoshi Yokoi[a,b,*]

[a] Drug Metabolism and Toxicology, Faculty of Pharmaceutical Sciences, Kanazawa University, Kakuma-machi, Kanazawa 920-1192, Japan
[b] Department of Drug Safety Sciences, Nagoya University School of Medicine, Nagoya 466-8550, Japan

ARTICLE INFO

Article history:
Received 16 November 2013
Received in revised form
25 December 2013
Accepted 13 February 2014
Available online 2 March 2014

Keywords:
miRNA
Drug-induced liver injury
Halothane
miR-106b
STAT3

ABSTRACT

MicroRNAs (miRNA) form a class of small non-coding RNA molecules that negatively regulate gene expression. Most cellular pathways are modulated by miRNAs. However, the pathophysiological role of miRNAs during drug-induced liver injury (DILI) remains largely unknown. In this study, the possible involvement of miRNAs in DILI caused by the hepatotoxic drug halothane (HAL) was investigated. Toward this purpose, miRNA microarray studies of HAL-induced liver injury were performed in mice at five different time points up to 24 h after dosing. To exclude any pharmacological effects on miRNA expression, isoflurane was used as a low hepatotoxic drug because it is structurally similar to HAL. Approximately 30–50% of the miRNA expression levels changed more than two-fold at every time point. *In silico* biological pathway analysis was performed to predict the targeted genes. Consequently, the miRNA gene down-regulation that occurred 1 h after HAL administration was primarily related to inflammation, immune systems and liver injury. Based on additional *in silico* analyses, we identified miR-106b. Subsequently target of miR-106b was investigated using liver samples from mice with HAL-induced liver injury. Among the predicted targets, we discovered that a signal transducer and activator of transcription 3 (STAT3) was particularly up-regulated beginning during the early phase of HAL-induced liver injury. Collectively, the suppressed miR-106b expression, as well as the subsequent up-regulation of STAT3, was critical for the pathogenesis of HAL-induced liver injury.

1. Introduction

Drug-induced liver injury is an adverse event that frequently leads to cessation of drug development, restrictions on drug use, and the withdrawal of approved drugs. Halothane (HAL) is an inhaled anesthetic that asymptomatically increases plasma transaminases in approximately 30% of patients and causes severe liver injury in limited numbers of patients (Ray and Drummond, 1991). HAL is metabolized by cytochrome P450 (CYP) 2E1 to form trifluoroacetyl (TFA)-chloride, which binds covalently to proteins and lipids. This TFA-adduct and/or HAL-modified macromolecule formation may initiate an immune response (Bourdi et al., 2001; Gut et al., 1993; Njoku et al., 1997).

A mouse model of HAL-induced liver injury was firstly established by You et al., 2006. Time-, mouse strain-, sex-dependent changes of serum ALT and AST and histopathological studies were previously investigated in detail (Kobayashi et al., 2009). The mechanism of HAL-induced liver injury involves immune responses, such as neutrophil infiltration, IL-17 induction, and natural killer cell stimulation (Cheng et al., 2010; Kobayashi et al., 2009; You et al., 2006), suggesting that many immune factors facilitate the development and progression of HAL-induced liver injury.

MicroRNAs (miRNAs) form a class of small non-coding RNAs that control gene expression by targeting mRNAs for translational repression or cleavage (Pillai, 2005; Zamore and Haley, 2005). Currently, more than 2000 and 1200 miRNAs have been identified in human and mice, respectively (http://www.mirbase.org/, version

Abbreviations: ACTB, β-actin; ALT, alanine aminotransferase; APAP, acetaminophen; CXCL1, chemokine (C-X-C motif) ligand 1; CYP, cytochrome P450; DILI, drug-induced liver injury; GAPDH, glyceraldehyde-3-phoshate dehydrogenase; Ct, cycle threshold; HAL, halothane; IL, interleukin; ISO, isoflurane; MAPK, mitogen-activated protein kinase; MIP-2, macrophage inflammatory protein 2; miRNA, microRNA; RORγt, RAR-related orphan receptor γt; STAT3, signal transducer and activator of transcription 3; TFA, trifluoroacetyl; Th, helper T; TNFα, tumor necrosis factor α; UTR, untranslated region.

* Corresponding author at: Department of Drug Safety Sciences, Nagoya University School of Medicine, Nagoya 466-8550, Japan. Tel.: +81 52 744 2110; fax: +81 52 744 2114.
E-mail addresses: sendo@stu.kanazawa-u.ac.jp (S. Endo), azu.y02@stu.kanazawa-u.ac.jp (A. Yano), tatsuki@p.kanazawa-u.ac.jp (T. Fukami), nmiki@p.kanazawa-u.ac.jp (M. Nakajima), tyokoi@med.nagoya-u.ac.jp, tyokoi@kenroku.kanazawa-u.ac.jp (T. Yokoi).

http://dx.doi.org/10.1016/j.tox.2014.02.011
0300-483X/

19); moreover, over 60% of human mRNAs might be targeted by miRNAs (Friedman et al., 2009). It has also been suggested that miRNAs are crucial for physiological and pathological processes (O'Connell et al., 2010; Takamizawa et al., 2004).

Recently, several reports concerning miRNA expression in relation to toxicological phenomena have been published and suggest that aberrant miRNA expression is involved in the progression of diseases, including cancer, heart disease, viral infections and inflammatory diseases (Bi et al., 2009; Latronico et al., 2008; Lee and Dutta, 2009; Nelson and Weiss, 2008; Wu et al., 2008). Additionally, various studies have investigated the major role of miRNAs in the response to environmental stressors, chemicals, and toxins (Chenand et al., 2013; Hou et al., 2011; Lema and Cunningham, 2010; Yokoi and Nakajima, 2013). Drug-metabolizing enzymes, such as those from the CYP family genes, are targeted by certain miRNAs (Komagata et al., 2009; Mohri et al., 2010; Tsuchiya et al., 2006). Xenobiotic and drug toxicities are also regulated by miRNAs. Tamoxifen is a potent hepatocarcinogen in rats that increases the expression of several oncogenic miRNAs (Pogribny et al., 2007). In liver fibrosis, miR-29 expression is suppressed in fibrotic liver tissue in humans and animals; miR-29 negatively regulates collagen production during liver fibrosis (Roderburg et al., 2011). Moreover, exposing rats to liver toxicants, such as acetaminophen or carbon tetrachloride, decreases the miR-298 and miR-370 expression levels, and the changes were observed during the early phases of toxicity; these miRNAs might regulate an oxidative stress-related gene (Fukushima et al., 2007). The liver-enriched miRNA species, such as miR-122 and miR-192, demonstrate high expression levels in plasma after APAP treatment, but their expression levels decreased in the liver (Wang et al., 2009). The expression level of both miRNAs in the liver changed significantly earlier than the plasma ALT levels, suggesting that these changes might be mechanistically important for drug-induced liver injury. However, miRNA expression has not been comprehensively studied during the early phase of hepatotoxicity caused by xenobiotics and drugs. In this study, we investigated whether miRNAs are involved in HAL-induced liver injury.

2. Materials and methods

2.1. Materials

HAL was purchased from Takeda Yakuhin (Osaka, Japan), and isoflurane (ISO) was obtained from Abbott Japan (Tokyo, Japan). Standard chow was obtained from Oriental Yeast (Tokyo, Japan). ReverTra Ace was purchased from Toyobo (Tokyo, Japan). RNAiso, Random hexamers and SYBR Premix Ex Taq were acquired from Takara (Shiga, Japan). Megaplex RT Primer Pool, TaqMan microRNA Reverse Transcription kit, TaqMan microRNA assays, TaqMan 2× Universal PCR Master Mix No AmpErase UNG and TaqMan Rodent MicroRNA Array v2.0 were purchased from Applied Biosystems (Foster City, CA). The Fuji Dri-Chem slides of GPT/ALT-PIII used to measure alanine aminotransferase (ALT) were obtained from Fuji Film Med (Tokyo, Japan). Rabbit polyclonal antibodies (anti-p38α mitogen-activated protein (MAP) kinase (MAPK14), anti-STAT3, and anti-Tyr705 phosphorylated STAT3) were purchased from Cell Signaling Technology (Beverly, MA). Rabbit polyclonal β-actin was purchased from BioVision (Mountain view, CA). IRDye 680 goat anti-rabbit IgG was obtained from LI-COR Biosciences (Lincoln, NE). All primers were commercially synthesized at Hokkaido System Sciences (Sapporo, Japan). All other chemicals and solvents were either analytical or the highest commercially available grade.

2.2. HAL-administration to mice

Female BALB/cCrSlc mice (8 weeks old, 18–23 g) were obtained from SLC Japan (Shizuoka, Japan). The animals were housed in polycarbonate cages using hardwood chip bedding in a controlled environment (temperature 25 ± 1 °C, humidity 50 ± 10%, and 12 h light/12 h dark cycle) in the institutional animal facility with access to a standard chow and water *ad libitum*. The animals were acclimatized for a week before being subjected to the experiments. The mice were intraperitoneally administered with 30 mmol/kg HAL dissolved in olive oil (100 mL/kg of body weight, $n = 5$). ISO was administered using the same dose as HAL ($n = 5$). Plasma and liver samples were collected 0.5, 1, 3, 6, 12 and 24 h after HAL administration. The plasma alanine aminotransferase (ALT) levels were determined using a Fuji Dri-Chem 4000 V (Fuji Film Med, Tokyo, Japan). The animals' maintenance and treatment were conducted in accordance with the National Institutes of Health Guide for Animal Welfare of Japan, and the protocol was approved by the Institutional Animal Care and Use Committee of Kanazawa University of Japan.

2.3. Real-time reverse transcription (RT)-PCR analysis

RNA from the mouse livers was isolated using RNAiso according to the manufacturer's instructions. Chemokine (C-X-C motif) ligand 1 (CXCL1), mitogen-activated protein kinase 14 (MAPK14), macrophage inflammatory protein 2 (MIP-2), RAR-related orphan receptor γt (RORγt), signal transducer and activator of transcription 3 (STAT3), tumor necrosis factor α (TNFα), and glyceraldehyde-3-phoshate dehydrogenase (GAPDH) were quantified using real-time RT-PCR. The primer sequences used in this study are listed in Table 1. The reverse transcription process and real-time RT-PCR were performed as previously described (Kobayashi et al., 2009).

2.4. TaqMan MicroRNA assay

The total RNAs, including the small RNAs from the liver, were isolated using RNAiso according to the manufacturer's instructions. The cDNAs were synthesized using TaqMan microRNA Reverse Transcription kit with the TaqMan microRNA assays 5× reaction mix according to the manufacturer's protocol. The cDNA sample were added to TaqMan 2× Universal PCR Master Mix (No AmpErase UNG) and TaqMan microRNA assays 5× reaction mix, and the real-time PCR was performed with a MP3000P (Stratagene, La Jolla, CA) and the MxPro QPCR software.

2.5. TaqMan MicroRNA array analysis

The total RNAs, including the small RNAs from the liver, were isolated using RNAiso according to the manufacturer's instructions. The cDNAs were synthesized from the total RNA using Megaplex RT Primer Pool A or B and TaqMan MicroRNA Reverse Transcription kit according to the manufacturer's protocol. The cDNA sample were added to TaqMan 2× Universal PCR Master Mix (No AmpErase UNG). The entire mixture was added to the individual ports of the TaqMan Array Rodent MicroRNA A + B Cards Set v2.0, which are 384-well microfluidics cards containing

Table 1
Sequences of the primers used in this study.

Target gene	Primer	Sequence
CXCL1	S	5′-GAT TCA CCT CAA GAA CAT CCA GAG-3′
	AS	5′-GAA GCC AGC GTT CAC CAG AC-3′
MAPK14	S	5′-GAA CGA AGA CTG TGA GCT CA-3′
	AS	5′-GAA ACA ACG TTC TTC CGG TC-3′
MIP-	S	5′-AAG TTT GCC TTG ACC CTG AAG-3′
2	AS	5′-ATC AGG TAC GAT CCA GGC TTC-3′
RORγt	S	5′-ACC TCC ACT GCC AGC TGT GTG CTG TC-3′
	AS	5′-TCA TTT CTG CAC TTC TGC ATG TAG ACT GTC CC-3′
STAT3	S	5′-TGC AGA GCA GGT ATC TTG AG-3′
	AS	5′-TGC TGC TTC TCT GTC ACT AC-3′
TNFα	S	5′-TGT CTC AGC CTC TTC TCA TTC C-3′
	AS	5′-TGA GGG TCT GGG CCA TAG AAC-3′
	S	5′-AAA TGG GGT GAG GCC GGT-3′
GAPDH	AS	5′-ATT GCT GAC AAT CTT GAG TGA-3′

S: sense primer, AS: antisense primer, CXCL1: chemokine (C-X-C motif) ligand 1, MAPK14: mitogen-activated protein kinase 14, MIP-2: macrophage inflammatory protein 2, RORγt: RAR-related orphan receptor γt, STAT3: signal transducer and activator of transcription 3, TNFα: tumor necrosis factor α, GAPDH: glyceraldehyde-3-phosphate dehydrogenase.

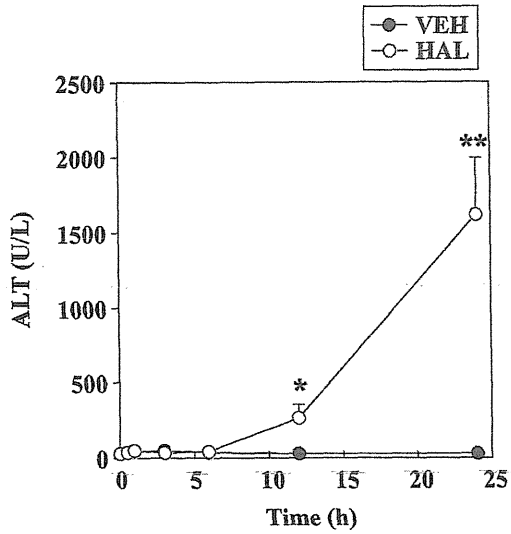

Fig. 1. Time-dependent changes in the plasma ALT levels in HAL-induced liver injury. Mice were administered intraperitoneally with 30 mmol/kg HAL. At 0, 0.5, 1, 3, 6, 12 and 24 h after the administration, blood samples were collected to assess the plasma ALT levels. Data are represented as the means ± SEM ($n = 4$). $^{*}P < 0.05$ and $^{**}P < 0.01$ relative to the VEH group at each time point. VEH: vehicle-treated group, HAL: halothane-treated group.

375 (A array) or 210 (B array) primer-probe sets for individual miRNAs. The miRNA expression was determined using quantitative real-time PCR with TaqMan Rodent MicroRNA array on a 7900HT Fast Real-Time PCR system (Life Technologies) using the manufacturer's recommended cycling conditions. The cycle threshold (Ct) values were calculated using the SDS software (v.2.4) with a baseline of 3–15 and an assigned minimum threshold of 0.2. The expression levels were evaluated using the comparative Ct method. The Ct values ranged from 0 to 40. The miRNAs that produced Ct values >35 in all groups were omitted from the data analysis because they may limit the RT efficiency, decreasing the sensitivity. The data were presented as (40-Ct). The ΔCt values [$\Delta Ct = (40\text{-}Ct_{HAL}) - (40\text{-}Ct_{VEH})$] were calculated as fold changes. The hierarchical clustering was performed using Cluster 3.0 software (complete linkage).

2.6. Immunoblot analysis

SDS-polyacrylamide gel electrophoresis and immunoblot analyses were performed according to Laemmli (Laemmli, 1970). Whole liver homogenates (30 μg) were separated on 10% polyacrylamide gels and electrotransferred onto polyvinylidene difluoride membranes (Immobilon-P (Millipore Corporation, Billerica, MA)). The membranes were probed with polyclonal antibodies (anti-MAPK14, anti-STAT3 or anti-Tyr705 phosphorylated STAT3) and a second corresponding fluorescent dye-conjugated antibody. An Odyssey Infrared Imaging system (LI-COR Biosciences, Lincoln, NE) was used for detection. The relative expression level was quantified using ImageQuant TL Image Analysis software (GE Healthcare, Little Chalfont, Buckinghamshire, UK). The MAPK14, STAT3 and Tyr705 phosphorylated STAT3 protein levels were normalized using the β-actin protein levels.

2.7. Statistical analysis

The data are presented as the means ± SEM. The comparisons between two groups were performed using a two-tailed Student's *t*-test. Differences with a value of $P < 0.05$ were considered statistically significant.

3. Results

3.1. Time-dependent changes of plasma ALT levels in HAL-induced liver injury in mice

The time-dependent changes in the plasma ALT levels after HAL administration were used to evaluate the liver injury in mice before studying the changes in the miRNA expression level induced by HAL treatment. Under the same dosing program reported by You et al., 2006, the mice were administered with HAL (30 mmol/kg, *i.p.*), generating a significant increase in their ALT levels 12 and 24 h after administration (Fig. 1). Histopathological study was conducted in the liver of HAL-administered mouse as previously reported (Kobayashi et al., 2009) (data not shown). In addition, there were no overt abnormalities in the plasma ALT levels of the HAL-administered mice until 6 h after administration (Fig. 1).

3.2. Time-dependent changes in the hepatic mRNA levels of cytokines in HAL-induced liver injury

To investigate whether HAL-induced liver injury affected the cytokine expression level, we measured the hepatic mRNA expression levels of the cytokines including CXCL1, MIP-2 and TNFα levels. The hepatic CXCL1, MIP-2 and TNFα mRNA levels were significantly increased 0.5 and 3 h, and 3 h and 1 h after the HAL administration, respectively (Fig. 2). Moreover, the CXCL1 expression peaked at 3 h; this result occurred earlier than that of the plasma ALT changes. These results suggested that immune-related responses participated in the early phases of HAL-induced liver injury.

3.3. Changes of hepatic miRNA expression at different time points after HAL administration

The expression profiles of the hepatic miRNAs 1, 3, 6, 12, and 24 h after HAL administration were measured using a TaqMan microRNA array. Over 200 miRNAs exhibited altered expression levels in each time point (Table 2). Based on the changes in their

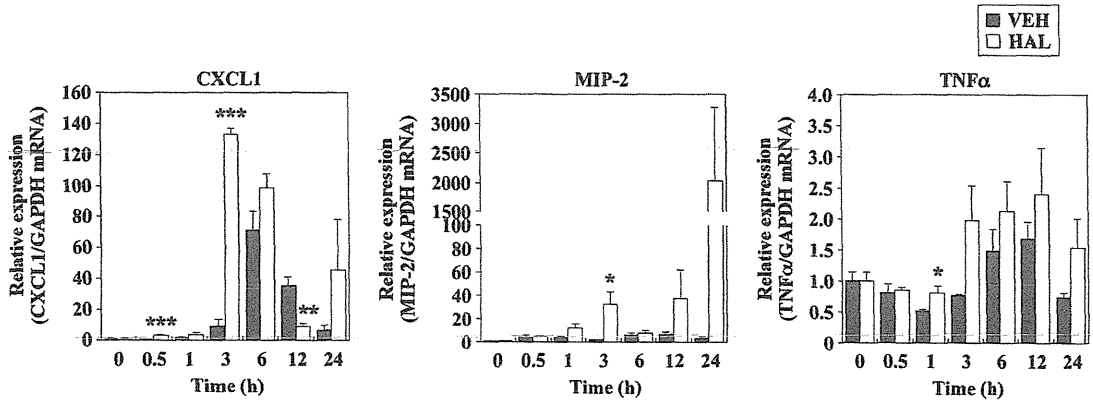

Fig. 2. Time-dependent changes in the hepatic mRNA expression levels during HAL-induced liver injury. Mice were administered intraperitoneally with 30 mmol/kg HAL. At 0, 0.5, 1, 3, 6, 12 and 24 h after the administration, the livers were collected to assess the expression levels of the hepatic mRNA. The hepatic mRNA's expression level was normalized to that of GAPDH. Data are represented as the means ± SEM ($n = 4$). Relative expression levels were calculated relative to non-treated mice. $^{*}P < 0.05$, $^{**}P < 0.01$ and $^{***}P < 0.001$ compared to the VEH group at each time point. VEH: vehicle-treated group, HAL: halothane-treated group.